HHS Public Access

Author manuscript

Sci Immunol. Author manuscript; available in PMC 2017 August 09.

Published in final edited form as:

Sci Immunol. 2017 March 03; 2(9): . doi:10.1126/sciimmunol.aag3160.

Maintenance of macrophage transcriptional programs and intestinal homeostasis by epigenetic reader SP140

Stuti Mehta[1], **D. Alexander Cronkite**[1], **Megha Basavappa**[1], **Tahnee L. Saunders**[1], **Fatemeh Adiliaghdam**[1], **Hajera Amatullah**[1], **Sara A. Morrison**[1], **Jose D. Pagan**[2], **Robert M. Anthony**[2], **Pierre Tonnerre**[1], **Georg M. Lauer**[1], **James C. Lee**[3], **Sreehaas Digumarthi**[1], **Lorena Pantano**[4], **Shannan J. Ho Sui**[4], **Fei Ji**[5], **Ruslan Sadreyev**[5], **Chan Zhou**[1], **Alan C. Mullen**[1], **Vinod Kumar**[6], **Yang Li**[6], **Cisca Wijmenga**[6], **Ramnik J. Xavier**[1], **Terry K. Means**[2], and **Kate L. Jeffrey**[1,*]

[1]Gastrointestinal Unit and Center for the Study of Inflammatory Bowel Disease, Massachusetts General Hospital, Harvard Medical School, Boston, MA 02114, USA [2]Center for Immunology and Inflammatory Diseases, Division of Rheumatology, Allergy and Immunology, Massachusetts General Hospital, Harvard Medical School, Charlestown, MA 02129, USA [3]Department of Medicine, University of Cambridge School of Clinical Medicine, Addenbrooke's Hospital, Cambridge, U.K [4]Department of Biostatistics, Harvard T.H. Chan School of Public Health, Boston, MA, USA [5]Department of Molecular Biology, Massachusetts General Hospital, Harvard Medical School, Boston, MA 02114, USA [6]Department of Genetics, University Medical Center Groningen, University of Groningen, Groningen, Netherlands

Abstract

Epigenetic "readers" that recognize defined posttranslational modifications on histones have become desirable therapeutic targets for cancer and inflammation. SP140 is one such bromodomain and plant homeodomain (PHD)–containing reader with immune-restricted expression, and single-nucleotide polymorphisms (SNPs) within *SP140* associate with Crohn's

*Corresponding author. kjeffrey@mgh.harvard.edu.

SUPPLEMENTARY MATERIALS

immunology.sciencemag.org/cgi/content/full/2/9/aag3160/DC1

Materials and Methods

References (*65–71*)

Author contributions: S.M. performed, analyzed, and interpreted most experiments and prepared the final figures with T.L.S. D.A.C performed Western blotting and assisted with patient PBMC and ChIP-seq experiments. M.B. performed lentivirus shRNA knockdown in mouse macrophages, siRNA knockdown in human macrophages, and qPCR. F.A., H.A., S.D., T.L.S., S.A.M., S.M., J.D.P., and R.M.A. performed DSS-colitis models and tissue analyses. P.T. and G.M.L. performed flow cytometry analysis of SP140 SNP patient PBMCs. L.P. and S.J.H.S. performed RNA-seq and ChIP-seq analyses. F.J. and R.S. performed ATAC-seq and SP140/H3K27me3/H3K4me3 quantitative relationship analyses. C.Z. and A.C.M. performed SP140, H3K27me3, and H3K27ac enhancer ranking analysis. J.C.L. performed SP140 expression analysis in intestinal biopsies. V.K., Y.L, and C.W. provided data from the BIOS Cohort. R.J.X. founded PRISM and interpreted experiments. T.K.M. performed and advised on mouse lentivirus shRNA–transduced bone marrow reconstitution experiments. S.M., D.A.C., M.B., L.P, S.J.H.S., F.A., H.A., T.L.S., and K.L.J. carried out statistical analyses. K.L.J. conceived, designed, supervised, and interpreted the experiments. K.L.J. wrote the final manuscript with input from S.M. and other authors.

Competing interests: The authors declare that they have no competing interests.

Data and materials availability: The microarray, RNA-seq, and ChIP-seq data reported in this paper are archived at the Gene Expression Omnibus Repository (www.ncbi.nlm.nih.gov/geo; accession no. GSE89876).

disease (CD). However, the function of SP140 and the consequences of disease-associated *SP140* SNPs have remained unclear. We show that SP140 is critical for transcriptional programs that uphold the macrophage state. SP140 preferentially occupies promoters of silenced, lineage-inappropriate genes bearing the histone modification H3K27me3, such as the *HOXA* cluster in human macrophages, and ensures their repression. Depletion of SP140 in mouse or human macrophages resulted in severely compromised microbe-induced activation. We reveal that peripheral blood mononuclear cells (PBMCs) or B cells from individuals carrying CD-associated SNPs within *SP140* have defective *SP140* messenger RNA splicing and diminished SP140 protein levels. Moreover, CD patients carrying *SP140* SNPs displayed suppressed innate immune gene signatures in a mixed population of PBMCs that stratified them from other CD patients. Hematopoietic-specific knockdown of *Sp140* in mice resulted in exacerbated dextran sulfate sodium (DSS)–induced colitis, and low *SP140* levels in human CD intestinal biopsies correlated with relatively lower intestinal innate cytokine levels and improved response to anti–tumor necrosis factor (TNF) therapy. Thus, the epigenetic reader SP140 is a key regulator of macrophage transcriptional programs for cellular state, and a loss of SP140 due to genetic variation contributes to a molecularly defined subset of CD characterized by ineffective innate immunity, normally critical for intestinal homeostasis.

INTRODUCTION

The epigenome is essential for generating signal-specific, cell lineage–specific, and kinetically precise gene expression in diverse cell types. Modifications on histones control the accessibility of DNA to transcription factors and serve as docking sites for epigenetic "reader" proteins that aid the assembly of transcriptional machinery complexes (1–4). Disruption of numerous epigenetic proteins culminates in malignant disease (5); however, our understanding of the role of altered epigenome regulators in nonmalignant, immune-driven disorders is relatively limited.

Epigenetic readers are structurally diverse proteins with evolutionarily conserved domains that dock to covalent modifications of histones, DNA, or transcription factors (6–8). They hold great promise as therapeutic targets in cancer and inflammation. For instance, members of the broadly expressed BET [bromodomain (the interaction module that reads ε-*N*-acetylation) and extraterminal] family perform central roles in translating histone modifications into context-specific transcription in cancer cells (9, 10), macrophages (1, 3, 11), and T cells (12, 13); show remarkable therapeutic tractability (3, 9); and are under investigation in several clinical trials (7, 14). However, the human proteome contains 46 bromodomain-containing proteins, each with defined affinities to certain histone acetylation sites (8), distinct tissue expression patterns, and unique protein interactors (4)—many of which remain uncharacterized. The bromodomain-containing protein SP140 is preferentially expressed in cells of the immune system (15), suggesting an immune-specific role for this epigenetic reader. Moreover, single-nucleotide polymorphisms (SNPs) within *SP140* have been significantly associated with immune disorders, such as Crohn's disease (CD) (16, 17), B cell chronic lymphocytic leukemia (CLL) (18), and multiple sclerosis (MS) (19), and autoantibodies against SP140 have been detected in patients with primary biliary cirrhosis

(20). Despite these findings, the function of SP140 and the consequence of disease-associated *SP140* SNPs have remained unknown.

SP140 belongs to the speckled protein (SP) family consisting of SP100, SP110, and SP140L, which have high sequence homology with the Autoimmune Regulator (AIRE) (21). SP family members are components of promyelocytic leukemia nuclear bodies (PML-NBs), which are ill-defined subnuclear structures regulated by a variety of cellular stresses [such as virus infection and interferon (IFN) and DNA damage], with implicated roles in many cellular processes, including higher-order chromatin organization (22). SP140 has several features indicative of a transcriptional regulator: an N-terminal HSR domain, a SAND domain [named after the few proteins (namely, SP100, AIRE, NucP41/P75, and DEAF) that have it] that interacts with DNA directly or through protein-protein interaction (23, 24), a plant homeodomain (PHD) that docks to histone methylation, and a bromodomain that binds acetylated histones (8). A potential transcriptional activator role for SP140 has been proposed (25).

Inflammatory bowel disease (IBD), including CD, is a complex disease involving inflammation of the gastrointestinal tract that is triggered by genetic, environmental, and possibly epigenetic factors (26, 27). Genome-wide association studies have identified more than 160 IBD-associated genetic variants (16), some of which have revealed the importance of competent and protective bacterial defense pathways elicited in response to commensal microbes in controlling intestinal homeostasis (26, 28–31). In this study, we investigated how an IBD-associated genetic variant of the epigenetic reader SP140 might impinge on defense responses to microbes that determine intestinal homeostasis.

We show that SP140 is a key orchestrator of transcriptional programs that support macrophage activation state attained in response to cytokines and microbes, through repression of lineage-inappropriate genes, including *HOX* genes. These SP140-dependent transcriptional programs are indispensable for intestinal and immune homeostasis, as the loss-of-expression consequences of CD-associated *SP140* SNPs we identified led to significantly suppressed innate immune gene signatures in a mixed population of peripheral blood mononuclear cells (PBMCs), which stratified CD patients carrying *SP140* SNPs from other CD patients not harboring *SP140* polymorphisms. Furthermore, hematopoietic-specific depletion of Sp140 in mice led to exacerbated dextran sulfate sodium–induced (DSS) colitis, and low *SP140* levels in human intestinal tissue correlated with relatively lower innate cytokine levels in diseased intestinal tissue and improved response to anti–tumor necrosis factor (TNF) therapy.

Thus, the epigenetic reader SP140 is central to the regulation of macrophage transcriptional programs critical to the establishment of intestinal homeostasis. This role of SP140 has direct relevance to human disease since a loss of SP140 by human genetic variation contributes to the development of CD.

RESULTS

SP140 is critical for mouse and human macrophage transcriptional programs

With the initial aim of identifying bromodomain-containing epigenetic readers that preferentially regulate immune cell function, we found SP140 to be selectively expressed in cells of the immune system (Fig. 1A) (15), with greatest abundance in mature B cells, dendritic cells, macrophages, and granulocytes and low amounts in hematopoietic stem cells (HSCs), monocytes, and T cells (fig. S1). SNPs within *SP140* have been associated with CD (16, 17), and SP family members have previously been identified as IFN-stimulated genes (ISGs) (32, 33). We therefore examined a potential role for SP140 in innate immune responses and inflammation. We found that *SP140* expression was high in both human M(IFN-γ) and mouse M[IFN-γ + lipopolysaccharide (LPS)] or M(LPS) macrophages, low in M[interleukin-4 (IL-4)] macrophages (Fig. 1, B and C), and up-regulated upon Toll-like receptor 2 (TLR2) or TLR4 activation (Fig. 1D and fig. S1). Short hairpin RNA (shRNA)–mediated knockdown of *Sp140* in mouse macrophages resulted in a significant down-regulation ($P < 0.05$, >1.5-fold) of almost 50% of all LPS-induced genes (Fig. 1E, fig. S2, and table S1), including transcripts that typically characterize M(LPS) activation status, such as the cytokines *Il6*, *Il1a*, *Il15*, *Tnfsf4*, and *Tnfsf15* and the chemokines *Cxcl10*, *Cxcl2*, *Ccl5*, *Ccl2*, *Ccl7*, *Ccl117*, and *Cxcl4*. The transcription factors *Nfkb2*, *Rel*, *Ear2*, *Ear3*, and *Ear10* and the chromatin modifiers or remodelers *Arid2*, *Hdac2*, and *Setd3* were also significantly down-regulated (Fig. 1E and table S1). A transient, small interfering RNA (siRNA)–mediated knockdown of *Sp140* with three separate siRNAs or a pool of four siRNA sequences in terminally differentiated macrophages (Fig. 1F, looks like fig. S2C, and Fig. 1G) also led to a significant reduction in *Il6*, *Tnf*, and *Ifnb1* transcripts after LPS stimulation (Fig. 1G and fig. S2) as well as IL-6 and TNF protein production (fig. S2). Similarly, *SP140* knockdown with a pool of four different siRNA sequences in human peripheral blood–derived macrophages resulted in a significant down-regulation of cytokines and cytokine receptors (*TNF*, *TNFSF9*, *CSF1*, *CSF3*, *IL3RA*, and *IL1RN*), chemokines (*CCL1*, *CCL20*, and *XCR1*), and transcription factors (*SMAD7*, *SMAD1*, and *NFATC1*) typically seen in LPS-induced macrophages differentiated with macrophage colony-stimulating factor (M-CSF) and IFN-γ (Fig. 1H and table S2). We also saw an uncharacteristic up-regulation of T cell receptor components (*CD3E*, *CD3D*, *CD3Z*, *CD247*, and *ITK*) in SP140 knockdown M(IFN-γ+LPS 4h) macrophages. This suggests that without SP140, correct macrophage identity or reprogramming under M-CSF/IFN-γ/LPS differentiating and activating conditions is significantly deviated. Gene set enrichment analysis (GSEA) of SP140-dependent genes revealed a significant down-regulation of a number of inflammatory or innate immune gene set signatures upon *SP140* knockdown and an up-regulation of Myc, E2F, and oxidative phosphorylation gene sets, where the latter is normally down-regulated because of the induction of aerobic glycolysis upon pathogen stimulation of macrophages (Fig. 1I) (34). Furthermore, ineffective activation of human macrophages with SP140 deficiency was confirmed by quantitative polymerase chain reaction (qPCR) of *IL6* and *TNF* transcripts in TLR4-stimulated macrophages from five independent donors (Fig. 1J). Thus, SP140 is a critical regulator of TLR4-induced transcriptional programs in mouse and human macrophages, and compromised *SP140* expression results in a significantly altered state of macrophage activation.

SP140 occupies transcriptional start sites in human macrophages

Bromodomain-containing proteins associate with chromatin by binding to acetylated histones or transcription factors (6–8). The SP140 bromodomain has a high but nonselective affinity for multiple acetylated histone peptide sites in vitro (8). However, SP140 also contains a SAND domain predicted to interact with DNA directly or through protein-protein interaction (23, 24) and a PHD that reads methylated histones (Fig. 2A). However, the PHD of SP140 may be atypical (35, 36). Nevertheless, there is no evidence to date demonstrating an association between SP140 and chromatin in cells. We conducted chromatin immunoprecipitation coupled with high-throughput sequencing (ChIP-seq) experiments to determine the global occupancy of endogenous SP140 in primary human macrophages M(IFN-γ) and M(IFN-γ+LPS 4h). This revealed a majority of SP140 occupancy at promoters (58.0%), defined as 5 kb upstream and downstream from the transcriptional start site (TSS) (Fig. 2B). SP140 was also found at enhancers (11.5%) [defined as regions greater than 5 kb from a TSS and marked with either H3K27ac or H3K4me1, or both (37)], within gene bodies (20.7%), and at distal intergenic regions (9.8%) (Fig. 2B), all of which did not change significantly upon the addition of LPS for 4 hours (fig. S3). Rank ordering of promoter SP140 occupancy in unstimulated and LPS-stimulated M(IFN-γ) macrophages revealed SP140 enrichment precisely at the TSS (Fig. 2C). The rank ordering of genes occupied by SP140 was altered upon LPS stimulation, but the TSS location was not (fig. S3). We next established a chromatin landscape for SP140 in human macrophages by using publicly available human macrophage ChIP-seq data for H3K4me3 to identify active or poised promoters, H3K27me3 to represent transcriptionally repressed regions, and H3K27ac or H3K4me1 to identify enhancers. Analysis of SP140 enrichment data as a metagene centered on the TSS revealed spatial colocalization of SP140 with H3K4me3 and H3K27me3 in promoters (Fig. 2D). We saw co-occupancy of promoter-bound SP140 (defined as peaks within TSS ± 5 kb) with H3K4me3 or H3K27me3 peaks, with more than 50% of all promoter-bound SP140 overlapping (within 0.5 kb) with regions marked by H3K4me3, H3K27me3, or a combination of these (fig. S4). We also observed SP140 overlap at inactive and active enhancers bearing H3K27ac, H3K4me1, or both marks (Fig. 2D and fig. S4) but no enrichment at “super-enhancers,” as defined by regions with the highest ranking of H3K27ac (fig. S5) (38). These results indicate that SP140 interacts with chromatin predominantly at gene promoter regions or TSS in human macrophages.

SP140 occupies repressed genes bearing H3K27me3 with inaccessible chromatin

Changes in H3K27me3 and H3K4me3 ratios on bivalent chromatin domains not only underlie cell-specific gene expression during differentiation but also enable fine-tuning of gene expression in differentiated cells (39). Therefore, we next examined quantitative relationships between SP140 and H3K27me3 or H3K4me3 in human macrophages. SP140 enrichment (ChIP-seq tag counts) positively correlated with H3K27me3 enrichment, with regions of highest SP140 occupancy being concentrated at high H3K27me3 and low H3K4me3, considered to be loci with low transcriptional activity ($\rho = 0.58$; $P < 1 \times 10^{-16}$) (Fig. 2, E and F). A correlation analysis of SP140 peak signal compared with ranked H3K27me3 ChIP peak signal values in human M(IFN-γ) and M(IFN-γ+LPS 4h) confirmed these findings ($\rho = 0.64$; $P < 2.2 \times 10^{-16}$) (fig. S6). We next performed assays for transposase-accessible chromatin (ATAC-seq) (40) in human M(IFN-γ) and M(IFN-γ+LPS

4h) macrophages and found that genes with the greatest SP140 occupancy (top 10% of SP140 ChIP peaks) showed markedly reduced chromatin accessibility at promoters compared with genes with low SP140 occupancy (bottom 10% of SP140 ChIP peaks) (Fig. 2G). We observed a similar trend of reduced chromatin accessibility at regions of high H3K27me3, a known repressive modification (fig. S7). Thus, SP140 preferentially occupies repressed genes with inaccessible chromatin and high H3K27me3 in human macrophages.

SP140 represses macrophage lineage-inappropriate genes, including HOX genes

To understand the functional significance of SP140 occupancy, we used the Genomic Regions Enrichment of Annotations Tool (GREAT) (41) and found the top gene families occupied by SP140 in human macrophages to be macrophage-inappropriate transcription factors. These included multiple homeobox (HOX) gene families, oligodendrocyte-specific basic helix-loop-helix transcription factors, forkhead box (FOX) family members, T-box transcription factors, and sex-determining region box (Fig. 3A and fig. S3). Upon siRNA-mediated knockdown of *SP140* in macrophages, we observed a marked increase in chromatin accessibility at the TSS of the top 10% of genes occupied by SP140 (Fig. 3B). The genes that showed increased chromatin accessibility were both up-regulated and down-regulated [greater than twofold; false discovery rate (FDR), <0.05] upon knockdown of *SP140*, as determined by RNA sequencing (RNA-seq) (Fig. 3C). However, genes with the greatest SP140 occupancy (top 5% of ChIP-seq peaks) showed a higher probability of being up-regulated upon depletion of SP140 (Fig. 3D), whereas those genes that were down-regulated did not (Fig. 3D), suggesting an indirect regulation of these genes by SP140.

We next focused on SP140 regulation of HOX genes, which include the HOXL, NKL, PRD, LIM, and SIX families, all of which were significantly overrepresented SP140 targets (Fig. 3A and fig. S3). Of all the *HOX* cluster genes, SP140 occupancy was highest at *HOXA9* (Fig. 3E), which is the most abundantly expressed *HOX* in HSCs, a known preserver of HSC self-renewal capacity, and is markedly down-regulated upon myeloid differentiation and macrophage activation (42). HOXA9 is also a known repressor of several genes controlling macrophage differentiation and function (43). At the *HOXA* cluster, SP140 preferentially occupied the "late" *HOXA7* to *HOXA13* cluster over the "early" *HOXA1* to *HOXA5* cluster in human M(IFN-γ) and M(IFN-γ+LPS 4h) macrophages (Fig. 3E). As reported in differentiated mouse macrophages (44), we found that human M(IFN-γ) macrophages expressed high *HOXA1* and low *HOXA9* (Fig. 3F, inset). A knockdown of *SP140* resulted in a significant up-regulation of *HOXA9* expression (Fig. 3G, looks like fig. S12A), assigning a repressive role to SP140 occupancy at *HOXA9*. Consistent with this, human and mouse macrophages with a knockdown of *SP140* and unrestrained *HOXA9*/*Hoxa9* were incapable of fully reprogramming after exposure to LPS (Fig. 1). Furthermore, depletion of both *SP140* and *HOXA9* restored expression of surface markers and cytokines, such as *CD11b*, *CSFR1*, and *IL6*, in human macrophages (Fig. 3H). Thus, through repression of lineage-inappropriate genes and particularly through repression of *HOXA9*, SP140 promotes the emergence and preservation of macrophage activation status.

CD-associated polymorphisms within *SP140* alter SP140 mRNA splicing

We examined the effect of the CD-associated *SP140* SNPs on *SP140* mRNA expression by RNA-seq of whole blood from individuals homozygous for the CD-risk SP140 SNP *rs7423615* ($SNP^{+/+}$, red) and sex-and age-matched controls ($SNP^{-/-}$, black). Multiple SNPs are in perfect linkage disequilibrium (LD) (r^2 ≥0.90; D' ≥0.98) with the top CD-associated intronic SNPs *rs7423615* and *rs6716753* (Fig. 4A) (16, 17), including those associated with CLL (rs13397985) (18) and MS (rs10201872) (19), and hence may act coordinately (hereafter collectively referred to as $SNP^{+/+}$). All of these SP140 SNPs are intronic, except for a single SNP in exon 7 (rs28445040) that was recently suggested to be the causal SNP (45). Of the five known protein-coding mRNA isoforms of *SP140* (Fig. 4B), we observed a selective and significant elevation in the expression of the *SP140* isoform ENST00000343805, which is devoid of exons 7 and 11, in peripheral blood from individuals carrying *SP140* risk alleles ($SNP^{+/+}$) (fig. S8). Similarly, we observed a specific and significant elevation of the *SP140* isoform ENST00000343805 as well as a reduction in the expression of the *SP140* isoforms ENST00000392045, 417495, 420434, and 373645 in PBMC RNA-seq data from the extensive BIOS Cohort (46), in individuals carrying one or two alleles of the CD-associated SP140 SNPs ($SNP^{-/+}$, $n = 206$; $SNP^{+/+}$, $n = 18$; $SNP^{-/-}$, $n = 428$) (Fig. 4C). The expression levels of a shorter *SP140* isoform (ENST00000373645) was unaffected, implicating SNPs further downstream in causing defective splicing of *SP140* (Fig. 4C). The splicing defect driven by disease-associated *SP140* SNPs was also observed in type I IFN and influenza-activated dendritic cells (fig. S8) (47). Furthermore, qPCR with exon-specific primers for *SP140* exons 1 and 7 confirmed low levels of exon 7 but equal levels of exon 1 in Epstein-Barr virus (EBV)–transformed B cells homozygous for the SP140 risk SNPs (Fig. 4D). Thus, our data show that the CD-associated SNPs within *SP140* alter *SP140* mRNA splicing, leading to elevated expression of the *SP140* isoform ENST00000343805 devoid of exons 7 and 11 and an overall reduction in total *SP140* mRNA expression.

Individuals carrying CD-associated *SP140* SNPs have reduced and truncated SP140 protein

We next examined how the CD-associated SP140 SNPs that disrupted mRNA splicing affect SP140 protein levels. Exons 7 and 11 of *SP140* do not code for any of the chromatin binding domains (SAND, PHD, and bromodomain) or nuclear localization sequence, but their exclusion is predicted to cause in-frame deletions of 26- and 33-amino acid peptide segments (~6.6 kDa) from the SP140 protein product. We assayed endogenous SP140 protein levels by immunoblot in EBV-immortalized B cell lines from individuals homozygous for *rs7423615* and associated SNPs (+/+) and observed a truncation of nuclear-localized SP140 protein isoforms (98- to 86-kDa isoforms) (Fig. 4E, looks like fig. S9C). Moreover, a pronounced loss of SP140 protein levels was evident (61 to 76% reduction in $SNP^{+/+}$ cells from Caucasian individuals and 11% reduction in $SNP^{+/+}$ cells from Sub-Saharan African individuals) (Fig. 4E), whereas expression of the related SP110 protein, whose genomic locus is adjacent to *SP140* and appears to share a divergent promoter, was unchanged (Fig. 4E). Hence, individuals homozygous for CD-associated SNPs within *SP140* have reduced protein levels of this epigenetic reader.

PBMCs carrying CD-associated SP140 SNPs have suppressed innate immune gene signatures

Given the identified role of SP140 in the maintenance of transcriptional programs that uphold macrophage differentiation and activation status and the mounting evidence of impaired homeostatic bacterial defense pathways in CD (26), we next assessed the consequence of the *SP140* CD-risk SNPs on the induction of innate immune responses in CD patients. We used global transcriptional profiling by RNA-seq to assess differentially expressed genes in PBMCs from healthy controls (HCs), CD patients not carrying *SP140* SNPs (CD^+ SP140 $SNP^{-/-}$), and CD patients homozygous for *SP140* SNPs (CD^+ SP140 $SNP^{+/+}$) before and after LPS stimulation. Similar to what we observed in EBV B cell lines, CD patients homozygous for *SP140* SNPs had a specific reduction in the expression of *SP140* exon 7 in whole blood and a marked loss of SP140 protein in PBMCs (Fig. 5, A and B, looks like fig. S12B). We did not observe any genotype-specific differences in the proportion, activation status, or type of leukocyte subsets within PBMCs, as assessed with flow cytometry using established surface markers (fig. S10). However, CD^+ *SP140* $SNP^{+/+}$ PBMCs showed a considerably enhanced deviation in gene expression from HCs compared with CD^+ *SP140* $SNP^{-/-}$ PBMCs (~1100 compared with ~350 differentially expressed genes, respectively) (Fig. 5C). The vast majority of CD^+ *SP140* $SNP^{+/+}$ differential genes were down-regulated compared with HCs (Fig. 5, D and E). Furthermore, only ~15% of the genes were differentially expressed in both $SNP^{+/+}$ and $SNP^{-/-}$ compared with HCs, demonstrating clearly molecularly defined and stratified subsets of CD (Fig. 5C and fig. S10). A number of genes (496 or 442) were differentially expressed between CD^+ *SP140* $SNP^{+/+}$ and CD^+ *SP140* $SNP^{-/-}$ PBMCs, most of which were down-regulated in CD^+ *SP140* $SNP^{+/+}$ (Fig. 5, C and D, fig. S10, and table S3). The genes that stratified *SP140* $SNP^{+/+}$ CD patients from other CD patients contain known HOXA9 targets (43) that are associated with macrophage differentiation status and identity (*CD300A*, *CD163*, *CSFR1*, *CD209*, *CD36*, *TLR4*, and *CCR1*) and were specifically down-regulated in *SP140* $SNP^{+/+}$ PBMCs at steady state. Upon LPS stimulation, a number of cytokines and chemokines such as *IL6*, *IL1A*, *IFNG*, *CXCL1*, *CCL1*, *CCL2*, and *CCL7* that define M(LPS) cells were uniquely down-regulated in *SP140* $SNP^{+/+}$ PBMCs (Fig. 5E and table S3). Unbiased GSEA of genes that stratified CD^+ *SP140* $SNP^{+/+}$ PBMCs from CD *SP140* $SNP^{-/-}$ PBMCs revealed inflammatory response, TNF–nuclear factor κB, type I IFN, type II IFN, and IL-6–Janus kinase–STAT3 (signal transducer and activator of transcription 3) gene sets as the most significantly down-regulated in CD^+ *SP140* $SNP^{+/+}$ PBMCs (Fig. 5F). Thus, CD patients homozygous for *SP140* SNPs stratify from other CD patients not carrying *SP140* SNPs by displaying suppressed innate immune signatures in a mixed population of PBMCs.

SP140 $SNP^{+/+}$ PBMCs have compromised TLR-induced cytokine production

We next measured cytokine production from CD patient PBMCs with (*SP140* $SNP^{+/+}$) or without (*SP140* $SNP^{-/-}$) *SP140* SNPs, stimulated ex vivo with TLR4 or TLR3 ligands, and observed notable *SP140* genotype–specific differences. PBMCs from SP140 $SNP^{+/+}$ patients produced significantly less *IL6* and *TNF* transcript after stimulation with LPS or polyinosinic-polycytidylic acid (PolyI:C) (Fig. 6A). We also observed significantly reduced secretion of cytokines IL-6, TNF, IL-12, IFN-γ, and IL-8, and CCL3 after TLR4 or TLR3 stimulation of PBMCs from CD^+ *SP140* $SNP^{+/+}$ patients and significantly reduced

production of IL-1β, CCL3, and IL-15 after TLR3 stimulation (Fig. 6, B and C). PBMCs from CD$^+$ *SP140 SNP*$^{+/+}$ patients displayed significantly enhanced production of IL-13, a type 2 cytokine involved in both beneficial tissue repair and pathological fibrosis (48), after TLR4 or TLR3 activation (Fig. 6D). Hence, a genetic loss of SP140 prevents proper transcriptional reprogramming in response to TLR activation. As a result, CD patients homozygous for CD-associated SNPs within *SP140* generate compromised innate immune responses, a known contributing factor to intestinal imbalance and inflammation (26), compared with other CD patients not carrying the *SP140* CD-risk allele.

Hematopoietic knockdown of mouse Sp140 exacerbates DSS-colitis

To determine whether a deficiency of Sp140 can drive intestinal inflammation in vivo, we performed an inducible shRNA-mediated hematopoietic depletion of *Sp140* in mice. Bone marrow that was lentivirally transduced with shSp140 or a control shRNA under an isopropyl-β-D-thiogalactopyranoside (IPTG)–inducible promoter was transferred to irradiated congenic hosts, and IPTG was administered to trigger shRNA transcription and *Sp140* depletion after full reconstitution of the hematopoietic system (Fig. 7A). Ficoll-isolated circulating PBMCs from mice reconstituted with shSp140-transduced bone marrow were CD45.1$^+$ (Fig. 7B) and *Sp140*-depleted (Fig. 7C). Furthermore, an immunoblot of splenic lysates confirmed hematopoietic depletion of Sp140 (Fig. 7D, looks like fig. S12C). We subjected the mice to a DSS model of colitis, a useful model for studying the contribution of the innate immune system to IBD. Mice with a hematopoietic-specific depletion of *Sp140* (Fig. 7, B and C) displayed exacerbated colitis symptoms, as evidenced by significantly more weight loss (Fig. 7E), higher disease activity scores (Fig. 7F), increased fecal lipocalin (Fig. 7G), and reduced colon length (Fig. 7, H and I), compared with control mice. In addition, SP140-depleted mice had increased intestinal permeability, as measured by fluorescein isothiocyanate (FITC)–dextran in the blood 4 hours after gavage administration (Fig. 7J), as well as increased bacterial load in mesenteric lymph nodes (Fig. 7K). Colonic explants from SP140-depleted mice had elevated cytokine production (Fig. 7L), and SP140-depleted mice had significantly increased serum IL-6 (Fig. 7M). Furthermore, SP140-depleted mice had significantly higher histopathology scores with a more severe loss of goblet cell morphology, a diffuse lymphocytic infiltrate to the level of the lamina submucosa, a thickening of the mucosa, and extensive edema (Fig. 7, N and O). Thus, expression and function of immune-restricted Sp140 is a requirement for intestinal homeostasis, and a loss of Sp140 drives intestinal inflammation.

Lower *SP140* expression in intestinal biopsies correlates with better response to anti-TNF therapy

Given that *SP140* SNP CD patients stratified from other CD patients by ineffective innate immunity and reduced cytokine production from PBMCs, we next examined whether *SP140* expression correlated with innate cytokine levels in the intestine of IBD patients and their responsiveness to anti-TNF therapy. About 20% of patients are primary nonresponders to anti-TNF therapy, and 31 to 38% will eventually fail therapy. One predictor of responsiveness is a lower baseline expression of TNF and other cytokines in the intestine (49). We mined transcript expression data of intestinal biopsies taken before or after anti-TNF (infliximab) therapy (50) and found significantly lower expression of *SP140* in

intestinal biopsies taken before treatment in patients who ultimately responded to anti-TNF (Fig. 8A). After anti-TNF treatment, *SP140* levels were further reduced in anti-TNF responders but remained elevated in anti-TNF nonresponders (Fig. 8A). Lower SP140 mRNA levels in intestinal biopsies of TNF responders were independent of the immune cell composition (fig. S11). We also found lower levels of many innate immune cytokines in intestinal biopsies of patients with low *SP140* expression compared with patients with high *SP140* expression (Fig. 8B). Moreover, Gene Ontology analysis of all genes that positively correlated with *SP140* expression in intestinal biopsies ($r^2 > 0.75$) revealed gene signatures associated with immune cell activation (Fig. 8C). Thus, *SP140* levels in intestinal biopsies correlate with the intestinal inflammatory state and are predictive of responsiveness to anti-TNF therapy.

DISCUSSION

Our current understanding of disrupted epigenetic programs in immune-mediated disease is limited. Here, we report on SP140, a previously uncharacterized immune-restricted epigenetic reader that has previously reported SNPs that associate with CD (16, 17), CLL (18), and MS (19). We show that individuals bearing CD-associated *SP140* SNPs, most of which are intronic and in perfect LD with *SP140* SNPs associated with CLL and MS, have alterations in *SP140* mRNA splicing that ultimately result in loss of SP140 protein, consistent with the findings from a recent publication (45). Consequently, CD patients deficient in this epigenetic reader exhibited hyporesponsive innate immune responses to bacteria or viral ligands that stratified them from other CD patients. The development of IBD is influenced by host genetics as well as dysbiosis and impaired handling of commensal bacteria and virus communities (16, 26). Our data now provide evidence that an inability to interpret the immune epigenome due to loss of SP140 contributes to IBD. Furthermore, it adds SP140 to a number of other IBD-associated genes (*NOD2*, *ATG16L1*, *GPR65*, and *AIM2*) that drive innate immunity in the intestine and whose loss or variation results in impaired barrier defense, decreased cytokine production, and an inability to maintain gut microbial balance, which ultimately enhances intestinal inflammation (26, 28–30, 51).

We demonstrate in human M(IFN-γ) and M(IFN-γ+LPS) macrophages that the bromodomain/PHD/SAND domain–containing SP140 interacts with chromatin, predominantly at promoters and primarily at silenced, lineage-inappropriate genes marked by H3K27me3, to orchestrate macrophage transcriptional programs both at steady state and in response to cytokines and microbes. The highest amount of SP140 was found at *HOX* genes, particularly *HOXA9*, a known promoter of stem-like state in HSCs and an inhibitor of macrophage differentiation (42, 43, 52). Our work thus reveals an essential role for the epigenome reader SP140 in the coordination of HOX gene expression in mature macrophages. Many other epigenetic regulators also contribute to the management of hematopoietic *HOX* gene expression (39). These include two opposing groups of histone methyltransferases: MLL (mixed-lineage leukemia) and the EZH2 subunit of PRC2, as well as the H3K27me3 demethylase JMJD3. Similar to what we observed after *SP140* knockdown, genetic deletion or chemical inhibition of JMJD3 resulted in significantly altered macrophage activation after exposure to helminth or bacteria (53, 54). Further work is warranted to understand how the elaborate epigenetic regulation of HOX genes functions

in a range of macrophage tissue subtypes and precisely at what stage of cellular differentiation and/or activation. We also found SP140 occupancy on several other lineage-determining transcription factors that are repressed in macrophages (the oligodendrocyte-specific basic helix-loop-helix transcription factors *OLIG1* to *OLIG3*; the FOX family members *FOXB1*, *FOXC2*, *FOXD2*, *FOXD3*, and *FOXG1*; and the paired box proteins *PAX2*, *PAX3*, *PAX5*, *PAX6*, *PAX8*, and *PAX9*). Therefore, we propose that by suppressing multiple lineage-inappropriate genes in differentiated macrophages, SP140 coordinates transcriptional output that defines the macrophage state, particularly after exposure to cytokines and microbial pathogen–associated molecular patterns.

Given that our study is the first to examine the function of the epigenetic reader SP140 in any detail, many questions of course remain unanswered. For instance, it remains unclear which reading domains (bromodomain, PHD, and/or SAND) render specificity of SP140 binding to chromatin. Furthermore, a nucleosome affinity purification assay did not identify SP140 as a direct interactor of methylated H3K27 nucleosomes, at least in HeLa cells (55). Therefore, SP140 may dock to repressed loci in macrophages via other yet-to-be identified histone modifications. Moreover, we found SP140 to also occupy active enhancers, the repertoire of which is highly cell type– and activation state–specific (37, 56). Hence, whether SP140 is solely a repressor or whether its function is altered when docked to enhancers, particularly through the bromodomain, ultimately to establish macrophage identity, needs to be investigated. Another limitation of our study is that experiments were performed in either mouse bone marrow–derived macrophages, human peripheral blood–derived macrophages, or PBMCs stimulated with bacterial or viral ligands. Future studies that probe the function of SP140 in immune cells that reside specifically within the intestine may provide greater insight into the precise role of this epigenetic reader in homeostatic immunity toward commensal microbes. Also, SP140 function in other immune cell types could certainly contribute to CD and should be considered. However, because SP140 shows only 54% amino acid homology between mouse and human, studies of this protein solely in mice will have limitations. In addition, given the association of SP140 SNPs with CLL and MS and the high expression of SP140 in B cells and dendritic cells, the investigation of SP140 function in these cells is warranted. However, microbiome alterations that affect innate immune pathways have been observed in MS patients (57), and other MS-associated mutations (e.g., in *TNFRSF1A*) block TNF, mirroring the clinical experience of MS patients where anti-TNF therapies can exacerbate disease (58). Therefore, a genetic deficiency of *SP140* could conceivably contribute to MS through a reduction in TNF and other innate cytokines and merits investigation. Last, given the growing evidence that epigenetic reprogramming dictates antigen-independent trained immunity and tolerance (6, 34), genetic variants of *SP140* or other epigenome regulatory enzymes may have a broader impact on an individual's immune status than currently appreciated.

Together, our findings identify the epigenetic reader SP140 as a critical regulator of macrophage function and innate immunity that enables intestinal homeostasis. Our work also uncovers a direct link between a loss of SP140 through genetic variation and IBD. Given the enthusiasm surrounding the therapeutic tractability of histone binding domains by chemical inhibitors (7), it is worth noting that our results suggest that targeting this particular bromodomain-containing epigenetic reader may not be desirable, at least in

subsets of CD (or CLL or MS) patients bearing *SP140* SNPs. Furthermore, this work has important implications for understanding how alterations in the epigenome and the interpretation of the epigenome via readers can drive immune-mediated disease, which may inform better therapeutic strategies.

MATERIALS AND METHODS

Study design

The human study population consisted of adult patients enrolled in the Prospective Registry in IBD Study at Massachusetts General Hospital (PRISM), a single-center ongoing patient registry that aims to understand the causes of IBD and factors affecting disease progression. Patients were approached during their regularly scheduled clinic visits at the Massachusetts General Hospital (MGH) Crohn's and Colitis Center. Study research coordinators obtained consent, and medical history was obtained and confirmed by review of the electronic medical record. Animal studies were conducted under protocols approved by the MGH Institutional Animal Care and Use Committee. All in vitro experiments with primary mouse or human macrophages included two to six biological replicates performed in triplicate, as indicated in the figure legends. All in vivo experiments were performed independently two times, with four to seven animals per group.

SP140 ChIP-seq and analysis

Sixty million naïve or LPS-stimulated (100 ng/ml for 4 hours) human M(IFN-γ) macrophages were cross-linked with 1% formaldehyde (Fisher Scientific) for 10 min at room temperature. Formaldehyde was quenched with 1.25 M glycine for 5 min at room temperature. Cells were scraped, washed in cold phosphate-buffered saline (PBS) containing protease inhibitors, and frozen. Nuclei were isolated using the truChIP kit (Covaris Inc.), and chromatin was sheared at 4°C, 140 W, and 200 cycles per burst with 10% duty factor for 8 min and 30 s (Covaris Inc.). Input fraction was saved (0.7%), and the remaining sheared chromatin was used for ChIP with a polyclonal SP140 antibody (HPA006162, Sigma) or an immunoglobulin G isotype control (Millipore) in immunoprecipitation buffer [0.1% Triton X-100, 0.1 M tris-HCl (pH 8), 0.5 mM EDTA, and 0.15 M NaCl in 1× Covaris D3 buffer] at 4°C, rotating overnight, followed by incubation with Dynabeads Protein G (10003D, Life Technologies) for 4 hours. The chromatin-bead-antibody complexes were then washed sequentially with three wash buffers of increasing salt concentrations and TE buffer. Chromatin was eluted using 1% SDS in Tris-EDTA. Cross-linking was reversed by incubation with ribonuclease A (Roche) for 1 hour at 37°C, followed by an overnight incubation at 65°C with Proteinase K (Roche). DNA was purified with the QIAquick PCR Purification Kit (28104, Qiagen). Libraries of input DNA and ChIP DNA were prepared from gel-purified >300–base pair (bp) DNA fragments. Samples were multiplexed and sequenced on an Illumina HiSeq 2500 in the rapid mode to obtain 50-bp single-ended reads.

Peak calling was carried out with bcbio_nextgen (http://gihub.com/chapmanb/bcbio-nextgen). Briefly, after quality assessment using FastQC (www.bioinformatics.babraham.ac.uk/projects/fastqc/), reads were trimmed using cutadapt version 1.9.1 (http://cutadapt.readthedocs.io/en/stable/) with a quality cutoff of 5 to remove

low-quality 3′ ends from reads, retaining reads with a minimum length of 25 bp. Trimmed reads were mapped against the UCSC hg19 reference genome using Bowtie 2 version 2.2.7 (59) with default parameters. Alignments were sorted and filtered to retain only uniquely mapping reads using sambamba version 0.5.9 (60). ChIP peaks were called using MACS2 version 2.1.0 with broad option (61) for the SP140 M(IFN-γ) and M(IFN-γ+LPS 4h) ChIP samples versus input control DNA. Furthermore, relevant H3K27ac (GSE54972), H3K4me1 (GSE31621), H3K4me3 (GSM1146439), and H3K27me3 (GSM1625982 and GSM1625986) ChIP-seq data from human monocyte-derived macrophages were obtained from the Gene Expression Omnibus and analyzed in the same way. We used the broad option for H3K27me3 chip data and default narrow peak parameters for H3K27ac, H3K4me1, and H3K4me3. In the case of H3K27ac, we followed similar preprocessing steps to those described in a previously published paper (62): (i) paired-end files were converted to single end by retaining one read of each proper pair and removing improperly paired reads, (ii) regions corresponding to ENCODE blacklisted sites were removed, and (iii) replicates were pooled by merging the BAM files before peak calling. Similarly, replicates for H3K4me3 were pooled, and peaks were called on the merged BAM files. To filter the set of peak calls for each data set and obtain higher confidence peaks, we plotted histograms of the fold enrichment (FE) values and defined the background to be the mode of the FE values, that is, the value that occurs most often. This resulted in a cutoff of 3 for H3K27me3, 3.5 for SP140 M(IFN-γ) and SP140 M(IFN-γ+LPS 4h), 5 for H3K27ac and H3K4me1, and 6 for H3K4me3.

Assay for transposase-accessible chromatin

Human M(IFN-γ) macrophages were left unstimulated [M(IFN-γ)] or stimulated with LPS (100 ng/ml for 4 hours) [M(IFN-γ+LPS 4h)] and subjected to ATAC-seq as previously described (40). Briefly, 50,000 cells were pelleted, resuspended in 50 μl of lysis buffer [10 mM tris-HCl (pH 7.4), 3 mM $MgCl_2$, 10 mM NaCl, and 0.1% NP-40 (CA-630, IGEPAL)], and immediately centrifuged at 500*g* for 10 min at 4°C. The nuclei pellets were resuspended in 50 μl of transposition buffer (25 μl of 2× 13 tagmentation DNA buffer, 22.5 μl of dH_2O, and 2.5 μl of Illumina Tn5 transposase) and incubated for 30 min at 37°C. Transposed DNA was purified with the MinElute PCR Purification Kit (Qiagen) and eluted in 10 μl of elution buffer (Qiagen). Barcoded ATAC-seq libraries were prepared as previously described and sequenced on an Illumina HiSeq 2500.

Hematopoietic depletion of Sp140 in mice

To allow for temporal control of shRNA expression in vivo, we used the TRC905 lentiviral vector (Broad Institute), whereby shRNA expression is under the control of an IPTG-inducible promoter. In this system, IPTG binds to the Lac I repressor protein, preventing it from binding to three Lac O repressor binding sites surrounding the U6 promoter required for shRNA expression (63). The shRNA target 21-nucleotide oligomer sequences were as follows: shGFP, GCAAGCTGACCCTGAAGTTCAT; mouse shSP140, GATGATTACTCTTGGTCATAT. Plasmids were purified with a QIAprep Maxiprep kit (Qiagen) and transfected into human embryonic kidney–293T cells along with pCMV-dR8.2 dvpr and pCMV-VSVG for the production of lentivirus. Bone marrow progenitor cells obtained from CD45.1 C57BL/6 donor mice were placed in 24-well tissue culture dishes (1

× 10^6 cells per well) and infected with 400 μl of unconcentrated shRNA lentiviral supernatant and polybrene (7.5 μg/ml) on day 1. Cells were spun for 30 min at 800*g* and placed in fresh medium containing 15% fetal bovine serum, IL-3 (20 ng/ml), IL-6 (50 ng/ml), and stem cell factor (SCF) (50 ng/ml). On day 2, the bone marrow cells were reinfected again. On day 3, puromycin (3 μg/ml) was added to the growth medium. On day 4, the cells were harvested and washed twice in PBS. For bone marrow transplantation, CD45.2 C57BL/6 recipient mice were irradiated with 131Cs at 10 gray on day 0 and injected retro-orbitally with 2.5 × 10^6 CD45.1 lentivirus–transduced bone marrow in 200 μl of Dulbecco's modified Eagle's medium, after which the mice were monitored for 6 weeks to allow for immune reconstitution. Six weeks after transplantation, blood was analyzed for reconstitution by measuring CD45.1 by flow cytometry. Next, we administered IPTG (1 mg intraperitoneally and 10 mM IPTG into the drinking water for 1 week) to induce the shRNA. All mice were maintained under specific pathogen–free conditions at the animal facility of MGH under a protocol approved by the Institutional Animal Care and Use Committee.

Statistical analysis

Comparisons and statistical tests were performed as indicated in each figure legend. Briefly, for comparisons of multiple groups over time or with two variables, a two-way analysis of variance (ANOVA) was used and corrected for multiple post hoc comparisons, comparing all groups to each other, all groups to a control, or selected groups to each other. For comparisons of multiple groups with only one variable, a one-way ANOVA was performed and corrected for multiple post hoc comparisons. For comparisons of two groups, two-tailed paired or unpaired *t* tests were used, except where indicated. Statistical analyses were performed in the GraphPad Prism software. A *P* value of less than 0.05 was considered significant, denoted as $*P \leq 0.05$, $**P \leq 0.01$, $***P \leq 0.001$, and $****P < 0.0001$ for all analyses. Correlation analyses for SP140 mRNA expression in individuals carrying none, one, or two alleles of SP140 SNPs and SP140 ChIP-seq data with various histone modifications were performed with Spearman ranking coefficients. FDR correction was performed for all RNA-seq data.

Supplementary Material

Refer to Web version on PubMed Central for supplementary material.

Acknowledgments

We thank the clinical research project managers of the Prospective Registry in IBD Study at MGH (PRISM); I. Rocano-Ponce and D. Zhernakova (University of Groningen) for assistance with eQTL analysis from the BIOS Cohort; and C. Ye and N. Hacohen (Broad Institute) for mining SP140 transcript data from their human dendritic cell cohort. We thank P. Peterson (University of Tartu, Estonia) for the mouse monoclonal SP140 antibody and Z. Levine and J. T. Prior in the Jeffrey laboratory for technical support. We thank MGH's Microarray and Next Generation Sequencing cores and the Broad Institute Genomics Platform. We thank R. Mostoslavsky, C. Mackay, and N. Nedelsky for critical reading of the manuscript.

Funding: This work was supported by the Center for the Study of Inflammatory Bowel Disease (CSIBD) Program grant P30DK043351 (K.L.J. and R.J.X.), NIH R01 AI07087 (K.L.J.), and the Kenneth Rainin Foundation (K.L.J). K.L.J is a Claflin Distinguished Scholar at the MGH. F.J. and R.S were supported by NIH P30 DK040561, and J.C.L. was supported by a Wellcome Trust Intermediate Clinical Fellowship (105920/Z/14/Z). Bioinformatics analyses (L.P. and S.J.H.S.) were supported in part by Harvard Catalyst, the Harvard Clinical and Translational

Science Center (NIH UL1 RR 025758 and financial contributions from participating institutions), and the Harvard Stem Cell Institute Center for Stem Cell Bioinformatics.

REFERENCES AND NOTES

1. Hargreaves DC, Horng T, Medzhitov R. Control of inducible gene expression by signal-dependent transcriptional elongation. Cell. 2009; 138:129–145. [PubMed: 19596240]
2. Jang MK, Mochizuki K, Zhou M, Jeong HS, Brady JN, Ozato K. The bromodomain protein Brd4 is a positive regulatory component of P-TEFb and stimulates RNA polymerase II-dependent transcription. Mol Cell. 2005; 19:523–534. [PubMed: 16109376]
3. Nicodeme E, Jeffrey KL, Schaefer U, Beinke S, Dewell S, Chung C-W, Chandwani R, Marazzi I, Wilson P, Coste H, White J, Kirilovsky J, Rice CM, Lora JM, Prinjha RK, Lee K, Tarakhovsky A. Suppression of inflammation by a synthetic histone mimic. Nature. 2010; 468:1119–1123. [PubMed: 21068722]
4. Dawson MA, Prinjha RK, Dittmann A, Giotopoulos G, Bantscheff M, Chan W-I, Robson SC, Chung C-W, Hopf C, Savitski MM, Huthmacher C, Gudgin E, Lugo D, Beinke S, Chapman TD, Roberts EJ, Soden PE, Auger KR, Mirguet O, Doehner K, Delwel R, Burnett AK, Jeffrey P, Drewes G, Lee K, PHuntly BJ, Kouzarides T. Inhibition of BET recruitment to chromatin as an effective treatment for MLL-fusion leukaemia. Nature. 2011; 478:529–533. [PubMed: 21964340]
5. Suvà ML, Riggi N, Bernstein BE. Epigenetic reprogramming in cancer. Science. 2013; 339:1567–1570. [PubMed: 23539597]
6. Mehta S, Jeffrey KL. Beyond receptors and signaling: Epigenetic factors in the regulation of innate immunity. Immunol Cell Biol. 2015; 93:233–244. [PubMed: 25559622]
7. Arrowsmith CH, Bountra C, Fish PV, Lee K, Schapira M. Epigenetic protein families: A new frontier for drug discovery. Nat Rev Drug Discov. 2012; 11:384–400. [PubMed: 22498752]
8. Filippakopoulos P, Picaud S, Mangos M, Keates T, Lambert JP, Barsyte-Lovejoy D, Felletar I, Volkmer R, Muller S, Pawson T, Gingras AC, Arrowsmith CH, Knapp S. Histone recognition and large-scale structural analysis of the human bromodomain family. Cell. 2012; 149:214–231. [PubMed: 22464331]
9. Filippakopoulos P, Qi J, Picaud S, Shen Y, Smith WB, Fedorov O, Morse EM, Keates T, Hickman TT, Felletar I, Philpott M, Munro S, McKeown MR, Wang Y, Christie AL, West N, Cameron MJ, Schwartz B, Heightman TD, La Thangue N, French CA, Wiest O, Kung AL, Knapp S, Bradner JE. Selective inhibition of BET bromodomains. Nature. 2010; 468:1067–1073. [PubMed: 20871596]
10. Delmore JE, Issa GC, Lemieux ME, Rahl PB, Shi J, Jacobs HM, Kastritis E, Gilpatrick T, Paranal RM, Qi J, Chesi M, Schinzel AC, McKeown MR, Heffernan TP, Vakoc CR, Bergsagel PL, Ghobrial IM, Richardson PG, Young RA, Hahn WC, Anderson KC, Kung AL, Bradner JE, Mitsiades CS. BET bromodomain inhibition as a therapeutic strategy to target c-Myc. Cell. 2011; 146:904–917. [PubMed: 21889194]
11. Belkina AC, Nikolajczyk BS, Denis GV. BET protein function is required for inflammation: Brd2 genetic disruption and BET inhibitor JQ1 impair mouse macrophage inflammatory responses. J Immunol. 2013; 190:3670–3678. [PubMed: 23420887]
12. Bandukwala HS, Gagnon J, Togher S, Greenbaum JA, Lamperti ED, Parr NJ, Molesworth AMH, Smithers N, Lee K, Witherington J, Tough DF, Prinjha RK, Peters B, Rao A. Selective inhibition of $CD4^+$ T-cell cytokine production and autoimmunity by BET protein and c-Myc inhibitors. Proc Natl Acad Sci USA. 2012; 109:14532–14537. [PubMed: 22912406]
13. Mele DA, Salmeron A, Ghosh S, Huang HR, Bryant BM, Lora JM. BET bromodomain inhibition suppresses T_H17-mediated pathology. J Exp Med. 2013; 210:2181–2190. [PubMed: 24101376]
14. Prinjha R, Tarakhovsky A. Chromatin targeting drugs in cancer and immunity. Genes Dev. 2013; 27:1731–1738. [PubMed: 23964091]
15. Bloch DB, de la Monte SM, Guigaouri P, Filippov A, Bloch KD. Identification and characterization of a leukocyte-specific component of the nuclear body. J Biol Chem. 1996; 271:29198–29204. [PubMed: 8910577]
16. Jostins L, Ripke S, Weersma RK, Duerr RH, McGovern DP, Hui KY, Lee JC, Schumm LP, Sharma Y, Anderson CA, Essers J, Mitrovic M, Ning K, Cleynen I, Theatre E, Spain SL, Raychaudhuri S, Goyette P, Wei Z, Abraham C, Achkar J-P, Ahmad T, Amininejad L, Ananthakrishnan AN,

Andersen V, Andrews JM, Baidoo L, Balschun T, Bampton PA, Bitton A, Boucher G, Brand S, Büning C, Cohain A, Cichon S, D'Amato M, Jong DD, Devaney KL, Dubinsky M, Edwards C, Ellinghaus D, Ferguson LR, Franchimont D, Fransen K, Gearry R, Georges M, Gieger C, Glas J, Haritunians T, Hart A, Hawkey C, Hedl M, Hu X, Karlsen TH, Kupcinskas L, Kugathasan S, Latiano A, Laukens D, Lawrance IC, Lees CW, Louis E, Mahy G, Mansfield J, Morgan AR, Mowat C, Newman W, Palmieri O, Ponsioen CY, Potocnik U, Prescott NJ, Regueiro M, Rotter JI, Russell RK, Sanderson JD, Sans M, Satsangi J, Schreiber S, Simms LA, Sventoraityte J, Targan SR, Taylor KD, Tremelling M, Verspaget HW, Vos MD, Wijmenga C, Wilson DC, Winkelmann J, Xavier RJ, Zeissig S, Zhang B, Zhang CK, Zhao H, Internationa IB Genetic Consortiu (IIBDGC). Silverberg MS, Annese V, Hakonarson H, Brant SR, Radford-Smith G, Mathew CG, Rioux JD, Schadt EE, Daly MJ, Franke A, Parkes M, Vermeire S, Barrett JC, Cho JH. Host–microbe interactions have shaped the genetic architecture of inflammatory bowel disease. Nature. 2012; 491:119–124. [PubMed: 23128233]

17. Franke A, McGovern DPB, Barrett JC, Wang K, Radford-Smith GL, Ahmad T, Lees CW, Balschun T, Lee J, Roberts R, Anderson CA, Bis JC, Bumpstead S, Ellinghaus D, Festen EM, Georges M, Green T, Haritunians T, Jostins L, Latiano A, Mathew CG, Montgomery GW, Prescott NJ, Raychaudhuri S, Rotter JI, Schumm P, Sharma Y, Simms LA, Taylor KD, Whiteman D, Wijmenga C, Baldassano RN, Barclay M, Bayless TM, Brand S, Büning C, Cohen A, Colombel J-F, Cottone M, Stronati L, Denson T, De Vos M, D'Inca R, Dubinsky M, Edwards C, Florin T, Franchimont D, Gearry R, Glas J, Van Gossum A, Guthery SL, Halfvarson J, Verspaget HW, Hugot J-P, Karban A, Laukens D, Lawrance I, Lemann M, Levine A, Libioulle C, Louis E, Mowat C, Newman W, Panés J, Phillips A, Proctor DD, Regueiro M, Russell R, Rutgeerts P, Sanderson J, Sans M, Seibold F, Steinhart AH, Stokkers PCF, Torkvist L, Kullak-Ublick G, Wilson D, Walters T, Targan SR, Brant SR, Rioux JD, D'Amato M, Weersma RK, Kugathasan S, Griffiths AM, Mansfield JC, Vermeire S, Duerr RH, Silverberg MS, Satsangi J, Schreiber S, Cho JH, Annese V, Hakonarson H, Daly MJ, Parkes M. Genome-wide meta-analysis increases to 71 the number of confirmed Crohn's disease susceptibility loci. Nat Genet. 2010; 42:1118–1125. [PubMed: 21102463]

18. Sillé FC, Thomas R, Smith MT, Conde L, Skibola CF. Post-GWAS functional characterization of susceptibility variants for chronic lymphocytic leukemia. PLOS ONE. 2012; 7:e29632. [PubMed: 22235315]

19. International Multiple Sclerosis Genetics Consortium; Beecham AH, Patsopoulos NA, Xifara DK, Davis MF, Kemppinen A, Cotsapas C, Shah TS, Spencer C, Booth D, Goris A, Oturai A, Saarela J, Fontaine B, Hemmer B, Martin C, Zipp F, D'Alfonso S, Martinelli-Boneschi F, Taylor B, Harbo HF, Kockum I, Hillert J, Olsson T, Ban M, Oksenberg JR, Hintzen R, Barcellos LF, Wellcome Trust Case Control Consortium (WTCCC), International IBD Genetics Consortium (IIBDGC). Agliardi C, Alfredsson L, Alizadeh M, Anderson C, Andrews R, Bach Søndergaard H, Baker A, Band G, Baranzini SE, Barizzone N, Barrett J, Bellenguez C, Bergamaschi L, Bernardinelli L, Berthele A, Biberacher V, Binder TMC, Blackburn H, Bomfim IL, Brambilla P, Broadley S, Brochet B, Brundin L, Buck D, Butzkueven H, Caillier SJ, Camu W, Carpentier W, Cavalla P, Celius EG, Coman I, Comi G, Corrado L, Cosemans L, Cournu-Rebeix I, Cree BAC, Cusi D, Damotte V, Defer G, Delgado SR, Deloukas P, di Sapio A, Dilthey AT, Donnelly P, Dubois B, Duddy M, Edkins S, Elovaara I, Esposito F, Evangelou N, Fiddes B, Field J, Franke A, Freeman C, Frohlich IY, Galimberti D, Gieger C, Gourraud P-A, Graetz C, Graham A, Grummel V, Guaschino C, Hadjixenofontos A, Hakonarson H, Halfpenny C, Hall G, Hall P, Hamsten A, Harley J, Harrower T, Hawkins C, Hellenthal G, Hillier C, Hobart J, Hoshi M, Hunt SE, Jagodic M, Jelčić I, Jochim A, Kendall B, Kermode A, Kilpatrick T, Koivisto K, Konidari I, Korn T, Kronsbein H, Langford C, Larsson M, Lathrop M, Lebrun-Frenay C, Lechner-Scott J, Lee MH, Leone MA, Leppä V, Liberatore G, Lie BA, Lill CM, Lindén M, Link J, Luessi F, Lycke J, Macciardi F, Männistö S, Manrique CP, Martin R, Martinelli V, Mason D, Mazibrada G, McCabe C, Mero I-L, Mescheriakova J, Moutsianas L, Myhr K-M, Nagels G, Nicholas R, Nilsson P, Piehl F, Pirinen M, Price SE, Quach H, Reunanen M, Robberecht W, Robertson NP, Rodegher M, Rog D, Salvetti M, Schnetz-Boutaud NC, Sellebjerg F, Selter RC, Schaefer C, Shaunak S, Shen L, Shields S, Siffrin V, Slee M, Sorensen PS, Sorosina M, Sospedra M, Spurkland A, Strange A, Sundqvist E, Thijs V, Thorpe J, Ticca A, Tienari P, van Duijn C, Visser EM, Vucic S, Westerlind H, Wiley JS, Wilkins A, Wilson JF, Winkelmann J, Zajicek J, Zindler E, Haines JL, Pericak-Vance MA, Ivinson AJ, Stewart G, Hafler D, Hauser SL, Compston A, McVean G, De Jager P, Sawcer SJ, McCauley JL.

Analysis of immune-related loci identifies 48 new susceptibility variants for multiple sclerosis. Nat Genet. 2013; 45:1353–1360. [PubMed: 24076602]

20. Granito A, Yang WH, Muratori L, Lim MJ, Nakajima A, Ferri S, Pappas G, Quarneti C, Bianchi FB, Bloch DB, Muratori P. PML nuclear body component Sp140 is a novel autoantigen in primary biliary cirrhosis. Am J Gastroenterol. 2010; 105:125–131. [PubMed: 19861957]
21. Gibson TJ, Ramu C, Gemünd C, Aasland R. The APECED polyglandular autoimmune syndrome protein, AIRE-1, contains the SAND domain and is probably a transcription factor. Trends Biochem Sci. 1998; 23:242–244. [PubMed: 9697411]
22. Lallemand-Breitenbach V, de Thé H. PML nuclear bodies. Cold Spring Harb Perspect Biol. 2010; 2:a000661. [PubMed: 20452955]
23. Bottomley MJ, Collard MW, Huggenvik JI, Liu Z, Gibson TJ, Sattler M. The SAND domain structure defines a novel DNA-binding fold in transcriptional regulation. Nat Struct Biol. 2001; 8:626–633. [PubMed: 11427895]
24. Waterfield M, Khan IS, Cortez JT, Fan U, Metzger T, Greer A, Fasano K, Martinez-Llordella M, Pollack JL, Erle DJ, Su M, Anderson MS. The transcriptional regulator Aire coopts the repressive ATF7ip-MBD1 complex for the induction of immunotolerance. Nat Immunol. 2014; 15:258–265. [PubMed: 24464130]
25. Bloch DB, Chiche JD, Orth D, de la Monte SM, Rosenzweig A, Bloch KD. Structural and functional heterogeneity of nuclear bodies. Mol Cell Biol. 1999; 19:4423–4430. [PubMed: 10330182]
26. Peloquin JM, Goel G, Villablanca EJ, Xavier RJ. Mechanisms of pediatric inflammatory bowel disease. Annu Rev Immunol. 2016; 34:31–64. [PubMed: 27168239]
27. Alenghat T, Osborne LC, Saenz SA, Kobuley D, Ziegler CGK, Mullican SE, Choi I, Grunberg S, Sinha R, Wynosky-Dolfi M, Snyder A, Giacomin PR, Joyce KL, Hoang TB, Bewtra M, Brodsky IE, Sonnenberg GF, Bushman FD, Won KJ, Lazar MA, Artis D. Histone deacetylase 3 coordinates commensal-bacteria-dependent intestinal homeostasis. Nature. 2013; 504:153–157. [PubMed: 24185009]
28. Cadwell K, Patel KK, Maloney NS, Liu TC, Ng ACY, Storer CE, Head RD, Xavier R, Stappenbeck TS, Virgin HW. Virus-plus-susceptibility gene interaction determines Crohn's disease gene *Atg16L1* phenotypes in intestine. Cell. 2010; 141:1135–1145. [PubMed: 20602997]
29. Lassen KG, Kuballa P, Conway KL, Patel KK, Becker CE, Peloquin JM, Villablanca EJ, Norman JM, Liu TC, Heath RJ, Becker ML, Fagbami L, Horn H, Mercer J, Yilmaz OH, Jaffe JD, Shamji AF, Bhan AK, Carr SA, Daly MJ, Virgin HW, Schreiber SL, Stappenbeck TS, Xavier RJ. Atg16L1 T300A variant decreases selective autophagy resulting in altered cytokine signaling and decreased antibacterial defense. Proc Natl Acad Sci USA. 2014; 111:7741–7746. [PubMed: 24821797]
30. Man SM, Zhu Q, Zhu L, Liu Z, Karki R, Malik A, Sharma D, Li L, Malireddi RK, Gurung P, Neale G, Olsen SR, Carter RA, McGoldrick DJ, Wu G, Finkelstein D, Vogel P, Gilbertson RJ, Kanneganti TD. Critical role for the DNA sensor AIM2 in stem cell proliferation and cancer. Cell. 2015; 162:45–58. [PubMed: 26095253]
31. Chu H, Khosravi A, Kusumawardhani IP, Kwon AHK, Vasconcelos AC, Cunha LD, Mayer AE, Shen Y, Wu WL, Kambal A, Targan SR, Xavier RJ, Ernst PB, Green DR, McGovern DP, Virgin HW, Mazmanian SK. Gene-microbiota interactions contribute to the pathogenesis of inflammatory bowel disease. Science. 2016; 352:1116–1120. [PubMed: 27230380]
32. Madani N, Millette R, Platt EJ, Marin M, Kozak SL, Bloch DB, Kabat D. Implication of the lymphocyte-specific nuclear body protein Sp140 in an innate response to human immunodeficiency virus type 1. J Virol. 2002; 76:11133–11138. [PubMed: 12368356]
33. Grötzinger T, Jensen K, Will H. The interferon (IFN)-stimulated gene *Sp100* promoter contains an IFN-γ activation site and an imperfect IFN-stimulated response element which mediate type I IFN inducibility. J Biol Chem. 1996; 271:25253–25260. [PubMed: 8810287]
34. Netea MG, Joosten LAB, Latz E, Mills KHG, Natoli G, Stunnenberg HG, O'Neill LAJ, Xavier RJ. Trained immunity: A program of innate immune memory in health and disease. Science. 2016; 352:aaf1098. [PubMed: 27102489]

35. Zucchelli C, Tamburri S, Quilici G, Palagano E, Berardi A, Saare M, Peterson P, Bachi A, Musco G. Structure of human Sp140 PHD finger: An atypical fold interacting with Pin1. FEBS J. 2014; 281:216–231. [PubMed: 24267382]

36. Zhang X, Zhao D, Xiong X, He Z, Li H. Multifaceted histone H3 methylation and phosphorylation readout by the plant homeodomain finger of human nuclear antigen Sp100C. J Biol Chem. 2016; 291:12786–12798. [PubMed: 27129259]

37. Heintzman ND, Hon GC, Hawkins RD, Kheradpour P, Stark A, Harp LF, Ye Z, Lee LK, Stuart RK, Ching CW, Ching KA, Antosiewicz-Bourget JE, Liu H, Zhang X, Green RD, Lobanenkov VV, Stewart R, Thomson JA, Crawford GE, Kellis M, Ren B. Histone modifications at human enhancers reflect global cell-type-specific gene expression. Nature. 2009; 459:108–112. [PubMed: 19295514]

38. Lovén J, Hoke HA, Lin CY, Lau A, Orlando DA, Vakoc CR, Bradner JE, Lee TI, Young RA. Selective inhibition of tumor oncogenes by disruption of super-enhancers. Cell. 2013; 153:320–334. [PubMed: 23582323]

39. Mosammaparast N, Shi Y. Reversal of histone methylation: Biochemical and molecular mechanisms of histone demethylases. Annu Rev Biochem. 2010; 79:155–179. [PubMed: 20373914]

40. Buenrostro JD, Giresi PG, Zaba LC, Chang HY, Greenleaf WJ. Transposition of native chromatin for fast and sensitive epigenomic profiling of open chromatin, DNA-binding proteins and nucleosome position. Nat Methods. 2013; 10:1213–1218. [PubMed: 24097267]

41. McLean CY, Bristor D, Hiller M, Clarke SL, Schaar BT, Lowe CB, Wenger AM, Bejerano G. GREAT improves functional interpretation of *cis*-regulatory regions. Nat Biotechnol. 2010; 28:495–501. [PubMed: 20436461]

42. Argiropoulos B, Humphries RK. *Hox* genes in hematopoiesis and leukemogenesis. Oncogene. 2007; 26:6766–6776. [PubMed: 17934484]

43. Huang Y, Sitwala K, Bronstein J, Sanders D, Dandekar M, Collins C, Robertson G, MacDonald J, Cezard T, Bilenky M, Thiessen N, Zhao Y, Zeng T, Hirst M, Hero A, Jones S, Hess JL. Identification and characterization of Hoxa9 binding sites in hematopoietic cells. Blood. 2012; 119:388–398. [PubMed: 22072553]

44. De Santa F, Totaro MG, Prosperini E, Notarbartolo S, Testa G, Natoli G. The histone H3 lysine-27 demethylase Jmjd3 links inflammation to inhibition of polycomb-mediated gene silencing. Cell. 2007; 130:1083–1094. [PubMed: 17825402]

45. Matesanz F, Potenciano V, Fedetz M, Ramos-Mozo P, del Mar Abad-Grau M, Karaky M, Barrionuevo C, Izquierdo G, Ruiz-Peña JL, Isabel García-Sánchez M, Lucas M, Fernández Ó, Leyva L, Otaegui D, Muñoz-Culla M, Olascoaga J, Vandenbroeck K, Alloza I, Astobiza I, Antigüedad A, Villar LM, Álvarez-Cermeño JC, Malhotra S, Comabella M, Montalban X, Saiz A, Blanco Y, Arroyo R, Varadé J, Urcelay E, Alcina A. A functional variant that affects exon-skipping and protein expression of *SP140* as genetic mechanism predisposing to multiple sclerosis. Hum Mol Genet. 2015; 24:5619–5627. [PubMed: 26152201]

46. Tigchelaar EF, Zhernakova A, Dekens JAM, Hermes G, Baranska A, Mujagic Z, Swertz MA, Muñoz AM, Deelen P, Cénit MC, Franke L, Scholtens S, Stolk RP, Wijmenga C, Feskens EJM. An introduction to LifeLines DEEP: Study design and baseline characteristics. bioRXiv. 2014; 2014

47. Lee MN, Ye C, Villani A-C, Raj T, Li W, Eisenhaure TM, Imboywa SH, Chipendo PI, Ann Ran F, Slowikowski K, Ward LD, Raddassi K, McCabe C, Lee MH, Frohlich IY, Hafler DA, Kellis M, Raychaudhuri S, Zhang F, Stranger BE, Benoist CO, De Jager PL, Regev A, Hacohen N. Common genetic variants modulate pathogen-sensing responses in human dendritic cells. Science. 2014; 343:1246980. [PubMed: 24604203]

48. Gieseck RL III, Ramalingam TR, Hart KM, Vannella KM, Cantu DA, Lu W-Y, Ferreira-González S, Forbes SJ, Vallier L, Wynn TA. Interleukin-13 activates distinct cellular pathways leading to ductular reaction, steatosis, and fibrosis. Immunity. 2016; 45:145–158. [PubMed: 27421703]

49. Siegel CA, Melmed GY. Predicting response to anti-TNF agents for the treatment of Crohn's disease. Therap Adv Gastroenterol. 2009; 2:245–251.

50. Arijs I, De Hertogh G, Lemaire K, Quintens R, Van Lommel L, Van Steen K, Leemans P, Cleynen I, Van Assche G, Vermeire S, Geboes K, Schuit F, Rutgeerts P. Mucosal gene expression of

antimicrobial peptides in inflammatory bowel disease before and after first infliximab treatment. PLOS ONE. 2009; 4:e7984. [PubMed: 19956723]

51. Lassen KG, McKenzie CI, Mari M, Murano T, Begun J, Baxt LA, Goel G, Villablanca EJ, Kuo SY, Huang H, Macia L, Bhan AK, Batten M, Daly MJ, Reggiori F, Mackay CR, Xavier RJ. Genetic coding variant in GPR65 alters lysosomal pH and links lysosomal dysfunction with colitis risk. Immunity. 2016; 44:1392–1405. [PubMed: 27287411]
52. Thorsteinsdottir U, Mamo A, Kroon E, Jerome L, Bijl J, Lawrence HJ, Humphries K, Sauvageau G. Overexpression of the myeloid leukemia-associated *Hoxa9* gene in bone marrow cells induces stem cell expansion. Blood. 2002; 99:121–129. [PubMed: 11756161]
53. Satoh T, Takeuchi O, Vandenbon A, Yasuda K, Tanaka Y, Kumagai Y, Miyake T, Matsushita K, Okazaki T, Saitoh T, Honma K, Matsuyama T, Yui K, Tsujimura T, Standley DM, Nakanishi K, Nakai K, Akira S. The Jmjd3-*Irf4* axis regulates M2 macrophage polarization and host responses against helminth infection. Nat Immunol. 2010; 11:936–944. [PubMed: 20729857]
54. Kruidenier L, Chung C-w, Cheng Z, Liddle J, Che KH, Joberty G, Bantscheff M, Bountra C, Bridges A, Diallo H, Eberhard D, Hutchinson S, Jones E, Katso R, Leveridge M, Mander PK, Mosley J, Ramirez-Molina C, Rowland P, Schofield CJ, Sheppard RJ, Smith JE, Swales C, Tanner R, Thomas P, Tumber A, Drewes G, Oppermann U, Patel DJ, Lee K, Wilson DM. A selective jumonji H3K27 demethylase inhibitor modulates the proinflammatory macrophage response. Nature. 2012; 488:404–408. [PubMed: 22842901]
55. Bartke T, Vermeulen M, Xhemalce B, Robson SC, Mann M, Kouzarides T. Nucleosome-interacting proteins regulated by DNA and histone methylation. Cell. 2010; 143:470–484. [PubMed: 21029866]
56. Lawrence T, Natoli G. Transcriptional regulation of macrophage polarization: Enabling diversity with identity. Nat Rev Immunol. 2011; 11:750–761. [PubMed: 22025054]
57. Jangi S, Jangi S, Gandhi R, Cox LM, Li N, von Glehn F, Yan R, Patel B, Antonietta Mazzola M, Liu S, Glanz BL, Cook S, Tankou S, Stuart F, Melo K, Nejad P, Smith K, Topçuolu BD, Holden J, Kivisäkk P, Chitnis T, De Jager PL, Quintana FJ, Gerber GK, Bry L, Weiner HL. Alterations of the human gut microbiome in multiple sclerosis. Nat Commun. 2016; 7:12015. [PubMed: 27352007]
58. Gregory AP, Dendrou CA, Attfield KE, Haghikia A, Xifara DK, Butter F, Poschmann G, Kaur G, Lambert L, Leach OA, Prömel S, Punwani D, Felce JH, Davis SJ, Gold R, Nielsen FC, Siegel RM, Mann M, Bell JI, McVean G, Fugger L. TNF receptor 1 genetic risk mirrors outcome of anti-TNF therapy in multiple sclerosis. Nature. 2012; 488:508–511. [PubMed: 22801493]
59. Langmead B, Salzberg SL. Fast gapped-read alignment with Bowtie 2. Nat Methods. 2012; 9:357–359. [PubMed: 22388286]
60. Tarasov A, Vilella AJ, Cuppen E, Nijman IJ, Prins P. Sambamba: Fast processing of NGS alignment formats. Bioinformatics. 2015; 31:2032–2034. [PubMed: 25697820]
61. Feng J, Liu T, Qin B, Zhang Y, Liu XS. Identifying ChIP-seq enrichment using MACS. Nat Protoc. 2012; 7:1728–1740. [PubMed: 22936215]
62. Reschen ME, Gaulton KJ, Lin D, Soilleux EJ, Morris AJ, Smyth SS, O'Callaghan CA. Lipid-induced epigenomic changes in human macrophages identify a coronary artery disease-associated variant that regulates *PPAP2B* expression through altered C/EBP-beta binding. PLOS Genet. 2015; 11:e1005061. [PubMed: 25835000]
63. Godec J, Cowley GS, Barnitz RA, Alkan O, Root DE, Sharpe AH, Haining WN. Inducible RNAi in vivo reveals that the transcription factor BATF is required to initiate but not maintain $CD8^+$ T-cell effector differentiation. Proc Natl Acad Sci USA. 2015; 112:512–517. [PubMed: 25548173]
64. Subramanian A, Tamayo P, Mootha VK, Mukherjee S, Ebert BL, Gillette MA, Paulovich A, Pomeroy SL, Golub TR, Lander ES, Mesirov JP. Gene set enrichment analysis: A knowledge-based approach for interpreting genome-wide expression profiles. Proc Natl Acad Sci USA. 2005; 102:15545–15550. [PubMed: 16199517]
65. Yu G, Wang LG, He QY. ChIPseeker: An R/Bioconductor package for ChIP peak annotation, comparison and visualization. Bioinformatics. 2015; 31:2382–2383. [PubMed: 25765347]
66. Lawrence M, Huber W, Pagès H, Aboyoun P, Carlson M, Gentleman R, Morgan MT, Carey VJ. Software for computing and annotating genomic ranges. PLOS Comput Biol. 2013; 9:e1003118. [PubMed: 23950696]

67. Whyte WA, Orlando DA, Hnisz D, Abraham BJ, Lin CY, Kagey MH, Rahl PB, Lee TI, Young RA. Master transcription factors and mediator establish super-enhancers at key cell identity genes. Cell. 2013; 153:307–319. [PubMed: 23582322]

68. Li H, Durbin R. Fast and accurate short read alignment with Burrows–Wheeler transform. Bioinformatics. 2009; 25:1754–1760. [PubMed: 19451168]

69. John S, Sabo PJ, Thurman RE, Sung MH, Biddie SC, Johnson TA, Hager GL, Stamatoyannopoulos JA. Chromatin accessibility pre-determines glucocorticoid receptor binding patterns. Nat Genet. 2011; 43:264–268. [PubMed: 21258342]

70. Ramírez F, Ryan DP, Grüning B, Bhardwaj V, Kilpert F, Richter AS, Heyne S, Dündar F, Manke T. deepTools2: A next generation web server for deep-sequencing data analysis. Nucleic Acids Res. 2016; 44:W160–W165. [PubMed: 27079975]

71. Mizoguchi E. Chitinase 3–like-1 exacerbates intestinal inflammation by enhancing bacterial adhesion and invasion in colonic epithelial cells. Gastroenterology. 2006; 130:398–411. [PubMed: 16472595]

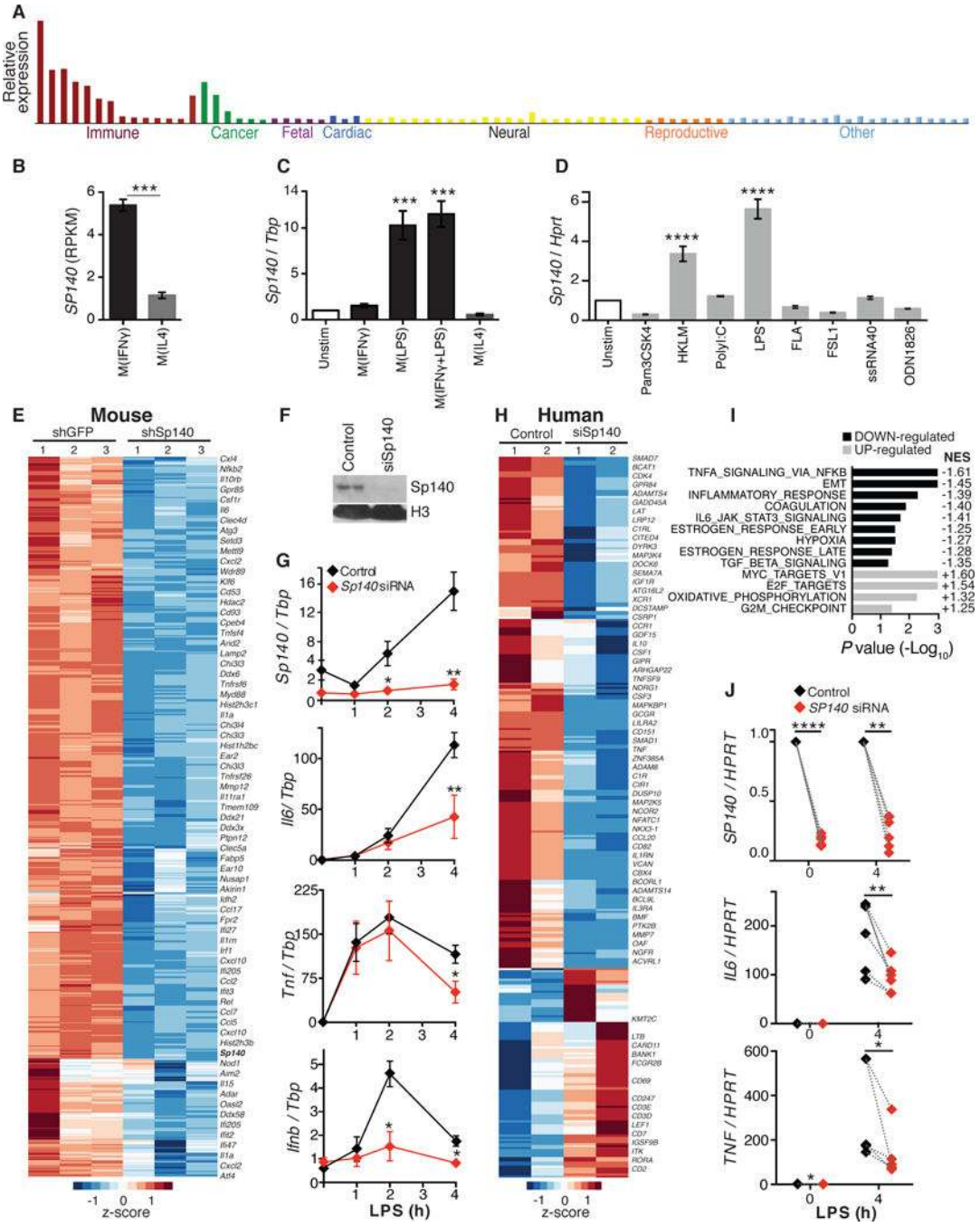

Fig. 1. The immune-restricted histone reader SP140 is essential for mouse and human LPS-induced macrophage transcriptional programs

(**A**) *SP140* expression in human tissues and cell types (BioGPS.org). (**B**) *SP140* expression in human M(IFN-γ) or M(IL-4) from GSE36952 ($n = 3$; ***$P < 0.001$, two-tailed unpaired t test). RPKM, reads per kilobase per million mapped reads. (**C**) Relative expression of mouse *Sp140* in indicated macrophage subsets ($n = 3$; ***$P < 0.001$, one-way ANOVA, post hoc Tukey's multiple comparisons test) and (**D**) in response to stimulation of mouse bone marrow–derived macrophages (BMDMs) with indicated TLR ligands, as measured by qPCR

(****$P < 0.0001$, one-way ANOVA, post hoc Tukey's multiple comparisons test). (**E**) Heat map of genes down-regulated (more than twofold; $n = 3$; $P < 0.05$) with shRNA-mediated *Sp140* knockdown in (LPS 4h)–stimulated BMDMs. (**F**) Expression of Sp140 protein in BMDMs as assessed by immunoblot. (**G**) *E*xpression of *Sp140*, *Il6*, *Tnf*, and *Ifnb* mRNA relative to *Tbp* in BMDMs transfected with siRNA against *Sp140* (red) or a control (black), and then stimulated with LPS (100 ng/ml) for the indicated times, as assessed by qPCR ($n =$ 3 to 4; *$P < 0.05$ and **$P < 0.01$, two-tailed, unpaired *t* test). (**H**) Heat map of genes down-regulated (more than twofold; $n = 2$; FDR <0.05) with *SP140* knockdown in (LPS 4h)–stimulated human M(IFN-γ) macrophages. (**I**) Hallmark gene sets significantly altered in *SP140* knockdown human M(IFN-γ+LPS 4h) macrophages, as assessed by GSEA (64). *P* values and normalized enrichment scores (NES) are indicated. (**J**) Expression of *SP140*, *IL6*, and *TNF* in human M(IFN-γ) macrophages, transfected with siRNA against *SP140* (red) or a control siRNA (black), and then stimulated with LPS (100 ng/ml for 4 hours). $n = 5$ to 6; *$P < 0.05$, **$P < 0.01$, and ****$P < 0.0001$, two-tailed paired *t* test. Error bars represent SEM.

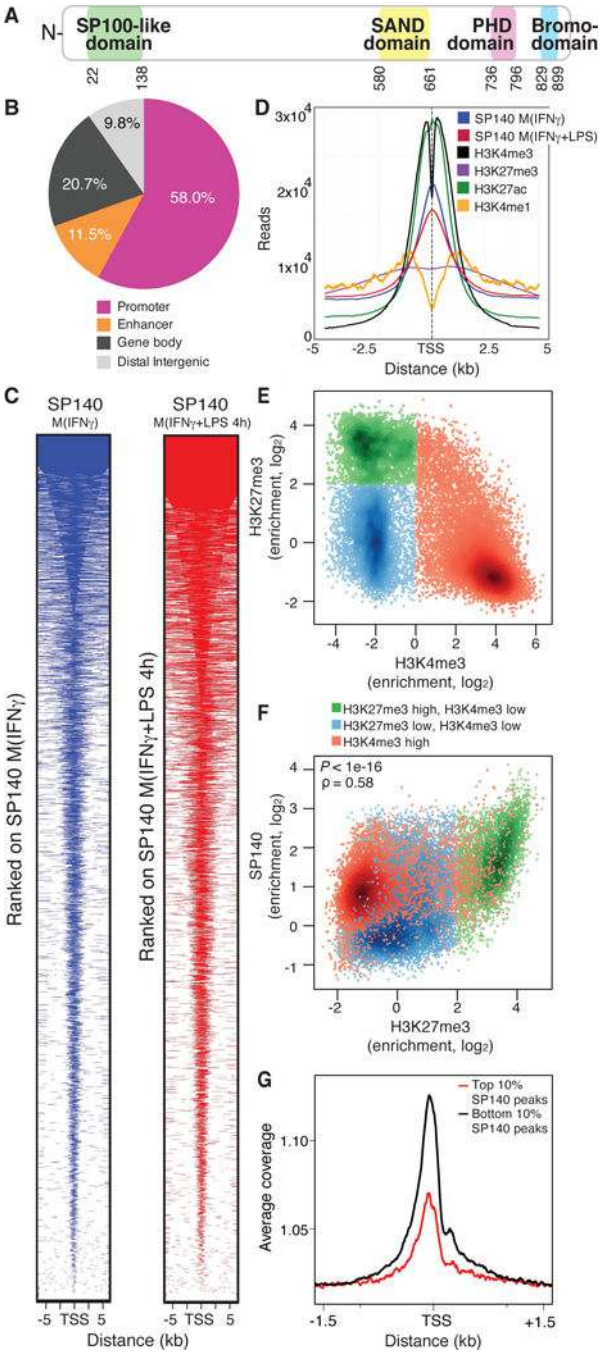

Fig. 2. SP140 preferentially interacts with chromatin at the TSS of inaccessible chromatin bearing repressive H3K27me3 in human M(IFN-γ) macrophages

(**A**) Schematic of predicted SP140 protein domains (UniProt). (**B**) Proportions of SP140 genome-wide occupancy at promoter regions (TSS ± 5 kb), enhancers (regions excluding TSS ± 5 kb marked with either H3K27ac or H3K4me1, or both), gene bodies, or distal intergenic regions in human M(IFN-γ) macrophages. (**C**) Heat map of SP140 ChIP-seq reads in unstimulated (blue) or LPS-stimulated (red) human M(IFN-γ) macrophages, rank-ordered from high to low occupancy centered on a ±5-kb window around the TSS. (**D**)

Metagene created from normalized genome-wide average reads for SP140, H3K4me3, H3K27me3, H3K27ac, and H3K4me1 centered on a TSS ± 5 kb window. (**E**) Quantitative relationship between ChIP-seq tag enrichment of H3K4me3 versus H3K27me3 in human macrophages. Each point is the ChIP tag count over input in TSS ± 3 kb regions, colored by levels of H3K27me3 or H3K4me3 enrichment. (**F**) Quantitative relationship between ChIP-Seq tag enrichment of SP140 versus H3K27me3, colored by levels of H3K27me3 or H3K4me3 enrichment. Spearman coefficient test rho (ρ) and *P* values are shown. (**G**) Average profiles of ATAC-seq tag density over TSS-proximal regions with the highest SP140 occupancy (top 10% ChIP-seq peaks) in M(IFN-γ) macrophages.

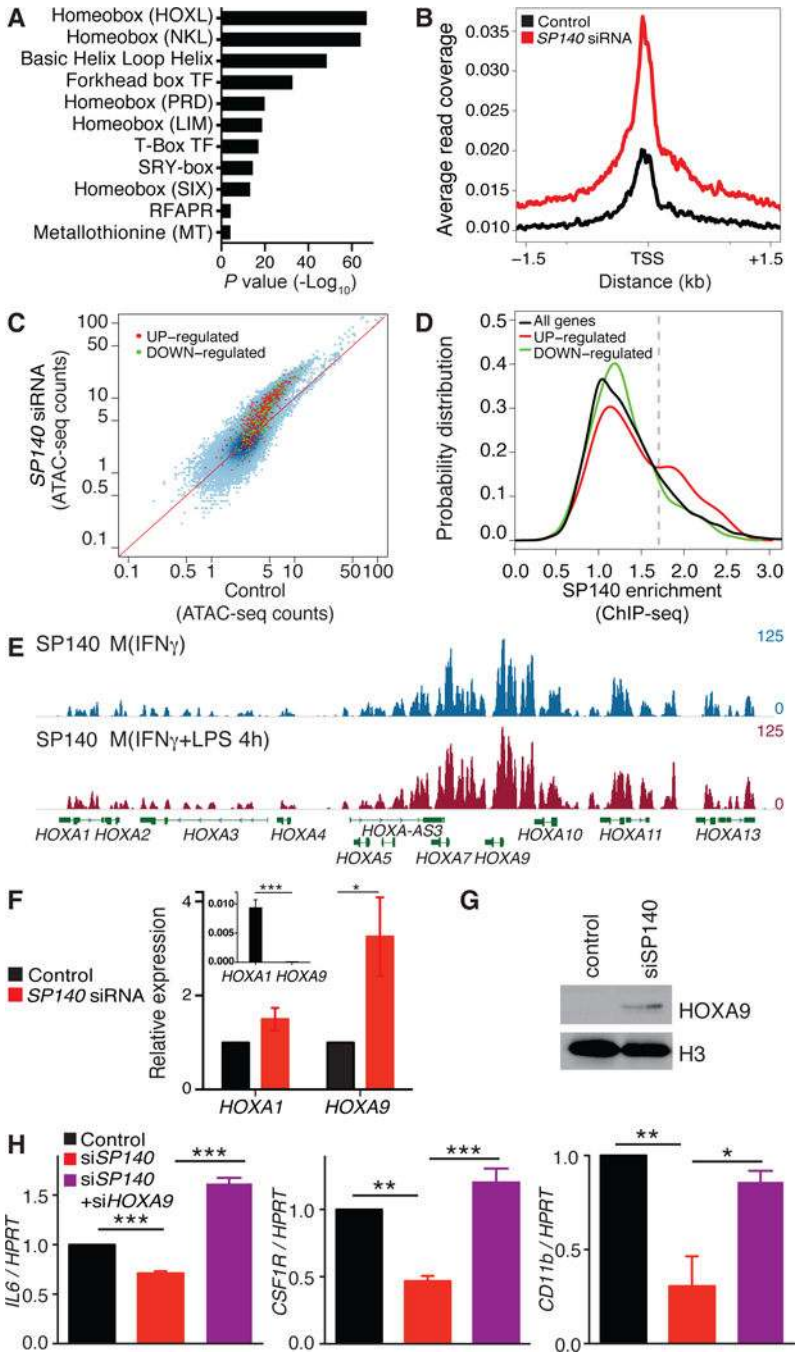

Fig. 3. SP140 silences human macrophage lineage-inappropriate genes, including HOX genes

(**A**) HUGO Gene Nomenclature Committee gene families most significantly represented in the top 10% SP140 ChIP-seq peaks in human M(IFN-γ) macrophages, as determined by GREAT (41). (**B**) Average profiles of ATAC-seq tag density over TSS-proximal regions with the highest (top 10%) SP140 occupancy, after SP140 knockdown in M(IFN-γ+LPS 4h) macrophages. (**C**) ATAC-seq counts (normalized counts per million) in control versus SP140 knockdown human M(IFN-γ+LPS) macrophages showing SP140-regulated genes identified by RNA-seq (red represents up-regulated and green represents down-regulated genes). (**D**)

Distribution (probability density function) of levels of SP140 enrichment (ChIP-seq) in the TSS-proximal region for all genes (black) compared with genes that were up-regulated (red) or down-regulated (green) in M(IFN-γ+LPS 4h) macrophages upon *SP140* knockdown. Top 5% SP140 enrichment among all genes is marked by a gray dashed line. (**E**) ChIP-seq tracks for SP140 across the ~15-kb *HOXA* gene cluster in human M(IFN-γ) (blue) or M(IFN-γ +LPS 4h) (red) macrophages. (**F**) Expression of *HOXA1* and *HOXA9* upon siRNA-mediated knockdown of *SP140*, relative to *HPRT* as determined by qPCR. Inset: Relative expression of *HOXA1* and *HOXA9* in human M(IFN-γ). Results represent the mean of two separate donors, performed in triplicate. $*P < 0.05$ and $***P < 0.001$, two-tailed unpaired *t* test. Error bars are SEM. (**G**) Immunoblot of HOXA9 protein upon siRNA-mediated knockdown of *SP140* in M(IFN-γ) macrophages. (**H**) Expression of *IL6*, *CSF1R*, and *CD11b* relative to *HPRT* upon siRNA-mediated knockdown of *SP140* and double knockdown of *SP140* and *HOXA9* in human M(IFN-γ) macrophages. Data are representative of two individual donors. $*P < 0.05$, $**P < 0.01$, and $***P < 0.001$, one-way ANOVA, Tukey's multiple comparison's test. Error bars are SEM.

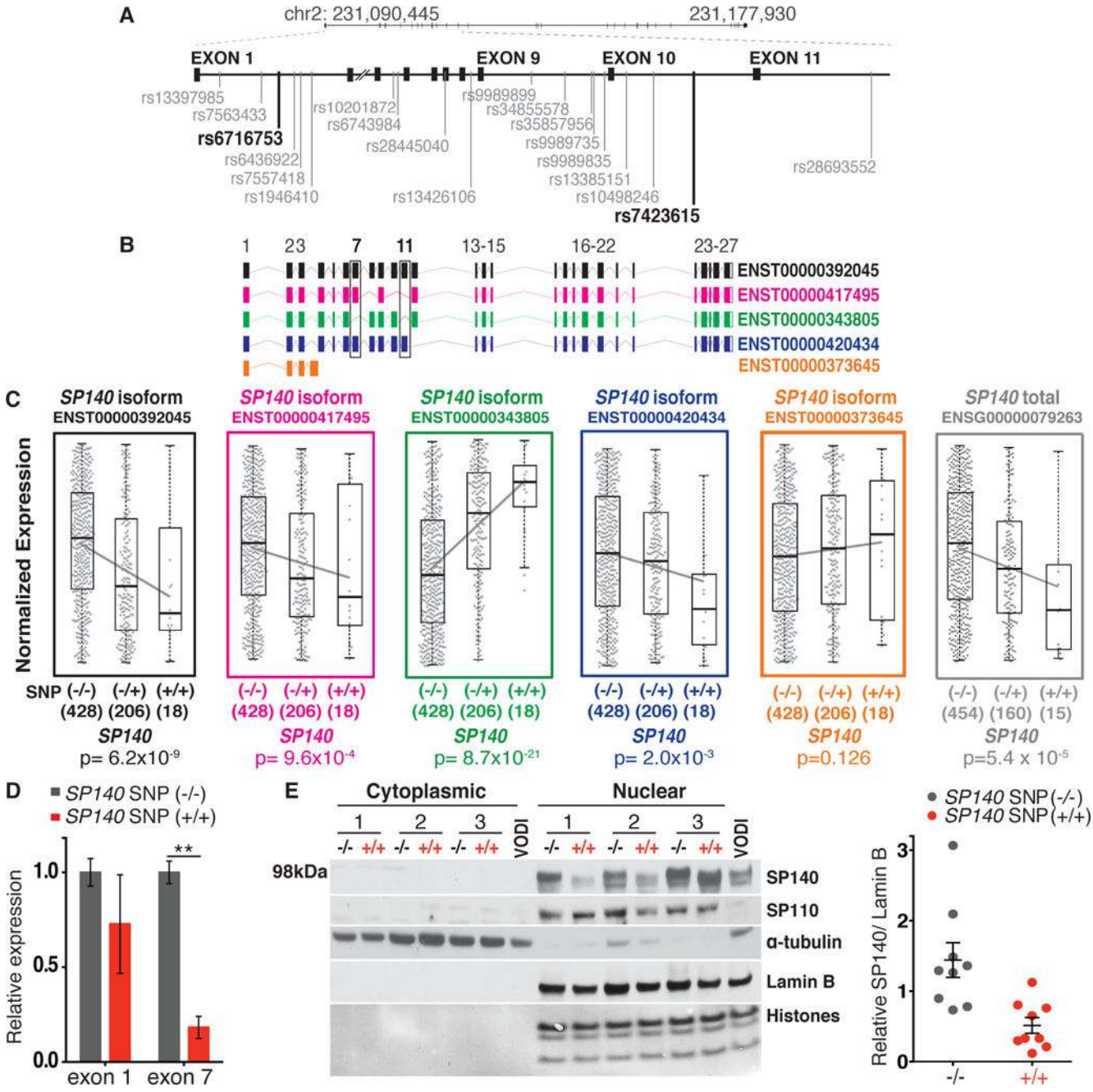

Fig. 4. Altered splicing of *SP140* mRNA and reduced SP140 protein in individuals carrying CD-associated *SP140* SNPs

(**A**) Location of the CD-associated SNPs *rs6716753* and *rs7423615* (in bold) in introns 1 and 10 of *SP140*, respectively (16, 17). All SNPs at the *SP140* locus that are in high LD (r^2 > 0.90; D' ≥0.98) with *rs6716753* and *rs7423615* are indicated. (**B**) Schematic of five protein-coding mRNA isoforms of *SP140* (Ensembl). Exon number is indicated. (**C**) Expression of *SP140* mRNA isoforms in individuals carrying no (–/–), one (–/+), or two (+/+) alleles of SP140 *rs7423615* SNPs (BIOS Cohort). Numbers of individuals, *P* values from Spearman correlation coefficients between expression levels, and genotypes are

indicated. (**D**) Expression levels of *SP140* exons 1 and 7 relative to the housekeeping gene *HPRT* as determined by qPCR in EBV-immortalized human B cell lines for the indicated *SP140* genotypes. $n = 3$; $^{**}P < 0.01$, two-tailed unpaired t test, Sidak-Bonferroni multiple testing correction. Error bars are SEM. (**E**) Left: Immunoblot analysis of SP140 and the related protein SP110 in cytoplasmic and nuclear fractions of EBV B cell lines with indicated *SP140* genotypes. Individuals in pairs 1 and 2 are Caucasian, whereas individuals in pair 3 are of Sub-Saharan African of Yoruba ancestry. α-Tubulin and Lamin B were used as loading controls for cytoplasmic and nuclear lysates, respectively. Ponceau stain of histones is shown. Veno-occlusive disease with immunodeficiency (VODI) EBV B cells deficient in SP110 serve as a control for SP110. Right: Quantification of SP140 relative to Lamin B (ImageJ). Error bars are SEM.

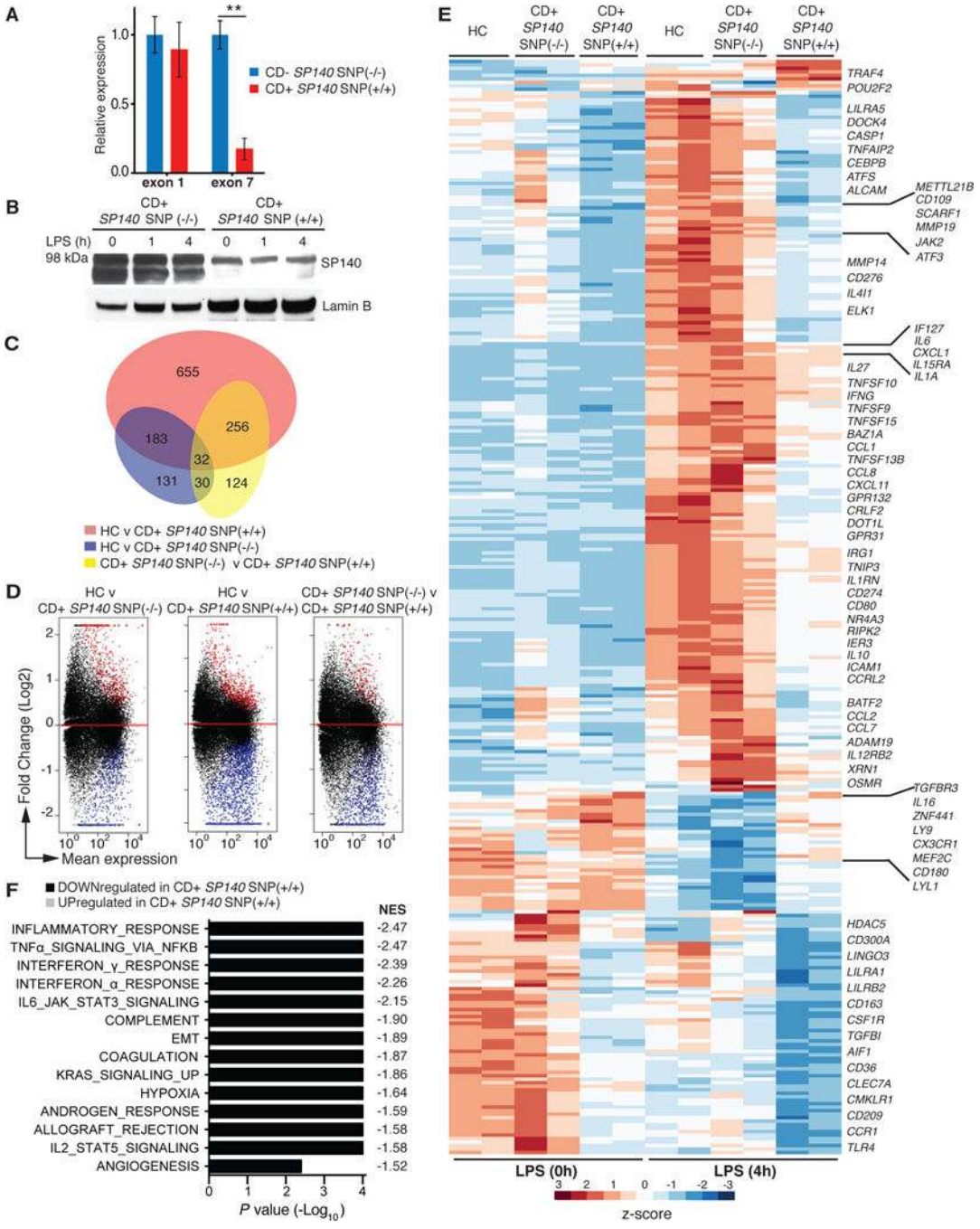

Fig. 5. Suppressed and stratified innate immune gene signatures in CD patient PBMCs carrying *SP140* SNPs

(**A**) Expression levels of *SP140* exons 1 and 7 relative to *HPRT* in PBMCs from individuals not carrying (SP140 SNP$^{-/-}$) or homozygous for *SP140* SNPs (+/+) ($n = 3$; $^{**}P < 0.01$, two-tailed unpaired *t* test, Sidak-Bonferroni multiple testing correction). Error bars are SEM. (**B**) Immunoblot of SP140 in PBMCs stimulated with LPS for the indicated times from CD patients with indicated *SP140* genotypes. Lamin B was used as a loading control. (**C**) Venn diagram of genes that were more than two fold differentially expressed (FDR, <0.05) in

unstimulated or LPS-stimulated (100 ng/ml for 4 hours) PBMCs from HCs versus CD^+ *SP140* $SNP^{-/-}$ (blue), HCs versus CD^+ *SP140* $SNP^{+/+}$ (red), and CD^+ *SP140* $SNP^{+/+}$ versus CD^+ *SP140* $SNP^{-/-}$ (yellow) ($n = 2$, RNA-seq). (**D**) MA plots showing genes that were more than twofold up-regulated (red) or more than twofold down-regulated (blue) in the indicated comparisons (FDR, <0.05). (**E**) Heat map of genes differentially expressed upon (LPS 4h) stimulation and showing a significant, more than twofold differential expression between CD^+ *SP140* $SNP^{+/+}$ and CD^+ *SP140* $SNP^{-/-}$ PBMCs (FDR, <0.05). (**F**) Hallmark gene sets significantly altered in CD^+ *SP140* $SNP^{+/+}$ as compared with CD^+ *SP140* $SNP^{-/-}$ PBMCs, as assessed by GSEA (64). *P* values calculated on the basis of 1000 gene set permutations (GSEA, Broad Institute) are shown.

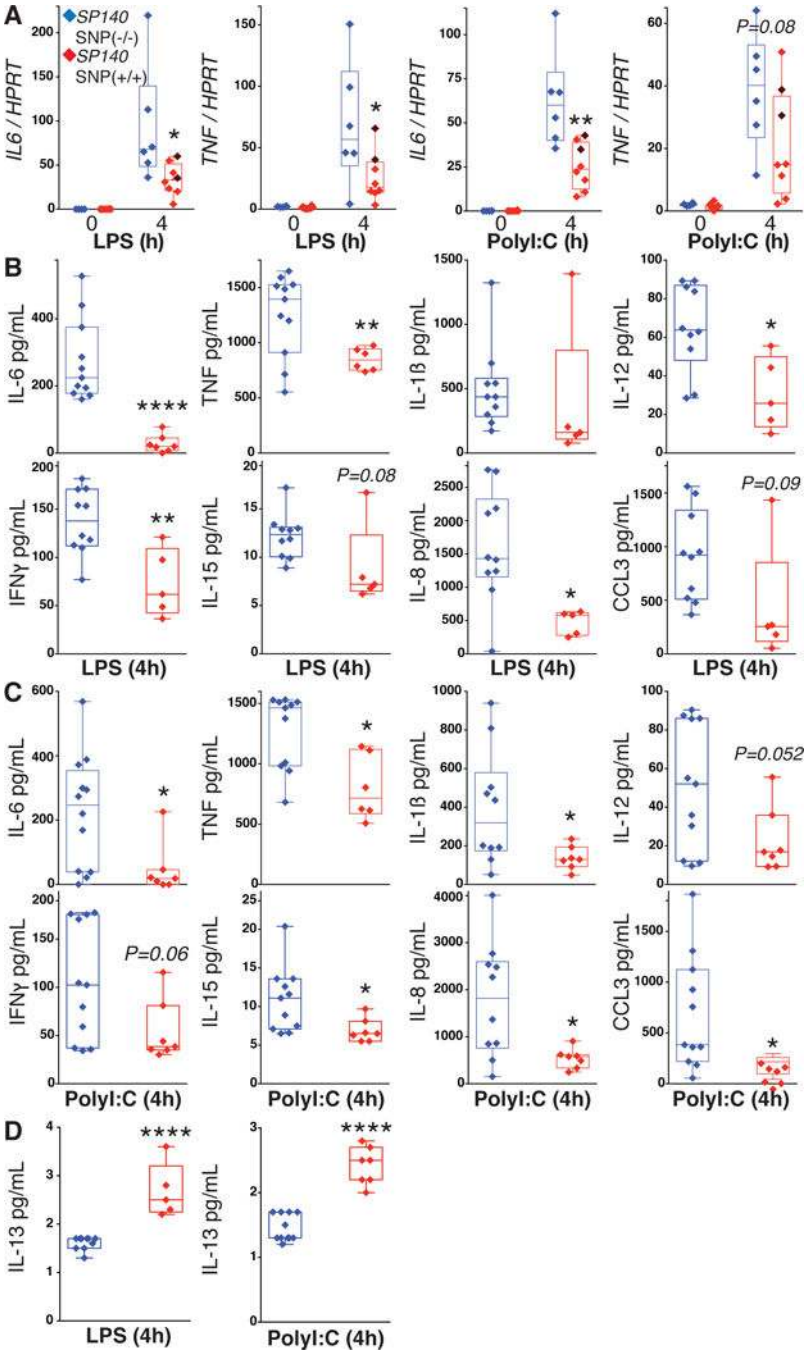

Fig. 6. Compromised cytokine secretion upon TLR stimulation by PBMCs from CD patients carrying CD-associated *SP140* SNPs

(**A**) Expression levels of *IL6* and *TNF* transcripts relative to *HPRT* control in CD$^+$ *SP140* SNP$^{-/-}$ ($n = 8$) or CD$^+$ *SP140* SNP$^{+/+}$ ($n = 6$) PBMCs after a 4-hour stimulation with LPS (100 ng/ml) or PolyI:C (10 μg/ml), as determined by qPCR. Dark red dots represent results from repeat blood biopsies from a patient obtained ~10 months apart. IL-6, TNF, IL-1β, IL-12, IFN-γ, IL-15, IL-8, and CCL3 production by PBMCs from CD$^+$ *SP140* SNP$^{-/-}$ ($n =$ 11; blue) and CD$^+$ *SP140* SNP$^{+/+}$ ($n = 7$; red) patients after a 4-hour stimulation ex vivo

with LPS (**B**) or PolyI:C (**C**) as measured by the Luminex Cytokine Human 25-Plex Panel. (**D**) IL-13 production by PBMCs from CD^+ *SP140* $SNP^{-/-}$ ($n = 11$; blue) and CD^+ *SP140* $SNP^{+/+}$ ($n = 7$; red) patients after a 4-hour stimulation ex vivo with LPS or PolyI:C. Data are represented as box-and-whisker plots showing the median and interquartile range (*$P < 0.05$, **$P < 0.01$, and ****$P < 0.0001$, two-tailed unpaired *t* test).

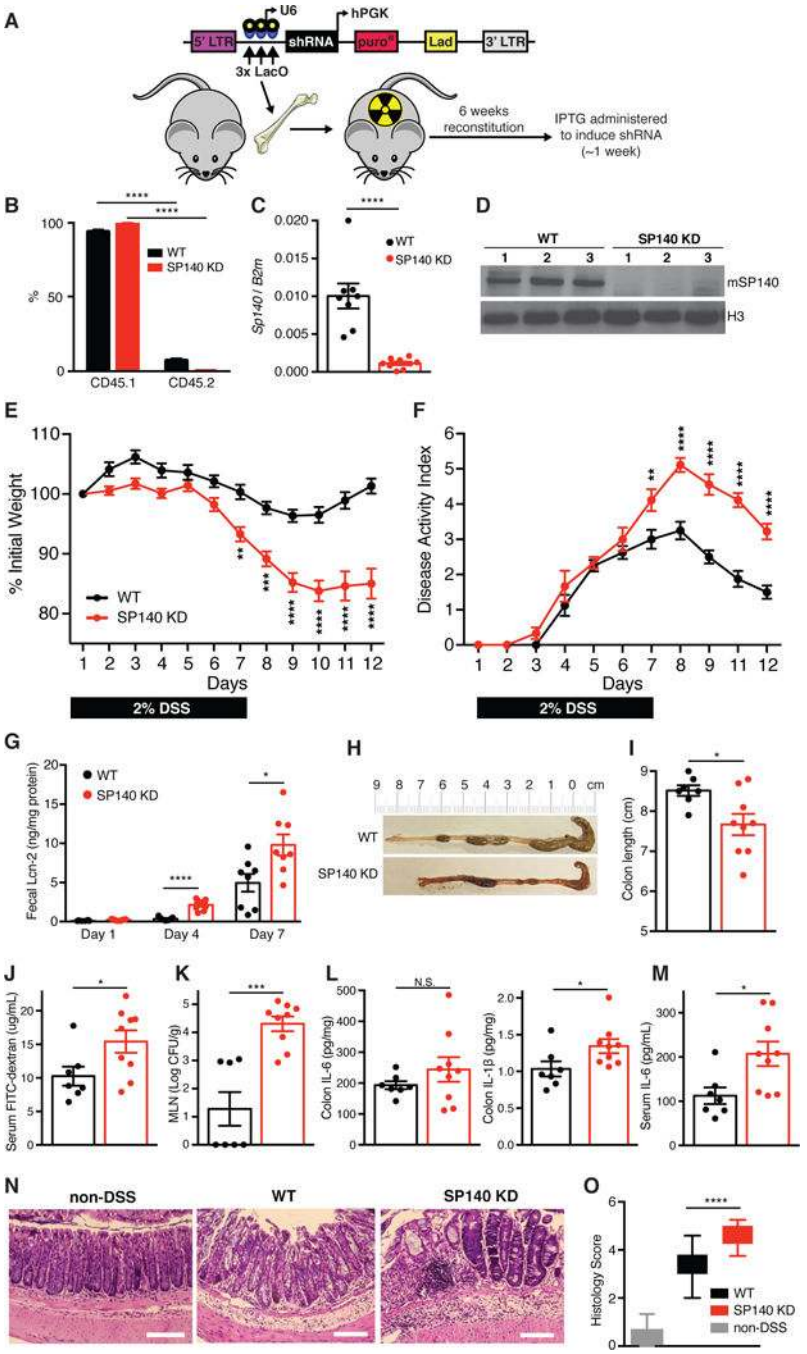

Fig. 7. Hematopoietic depletion of *Sp140* results in exacerbated DSS-induced colitis

(**A**) Schematic of IPTG-inducible shRNA knockdown (KD) in the hematopoietic system of mice. LTR, long terminal repeat. (**B**) Proportion of CD45.1$^+$ or CD45.2$^+$ cells in peripheral blood as determined by flow cytometry. (**C**) *Sp140* expression as assessed by qPCR in mononuclear cells isolated by Ficoll, normalized to β2-microglobulin, or (**D**) immunoblot of splenic lysates from irradiated CD45.2 mice reconstituted 6 weeks prior with control (shGFP) or *Sp140* knockdown (shSp140) CD45.1 bone marrow. Histone 3 serves as a loading control. (**E**) Daily body weight and (**F**) disease activity index measurements in wild-

type (WT) and *Sp140* knockdown mice after 2% DSS administration. (**G**) Fecal lipocalin-2 (Lcn-2) content at the indicated days after DSS administration. (**H**) Representative gross morphology images of WT and *Sp140* knockdown colons at day 12 after 2% DSS administration. (**I**) Quantification of colon lengths. (**J**) FITC levels in day 12 serum of WT and *Sp140* knockdown mice after 4 hours of intragastric FITC administration. (**K**) Bacterial burden in mesenteric lymph nodes (MLN) at day 12, expressed as log of colony-forming units (CFU) normalized to tissue weight. (**L**) IL-6 and IL-1β levels in day 12 colonic explant supernatants cultured for 24 hours. N.S., not significant. (**M**) IL-6 levels in serum of WT and *Sp140* knockdown mice at day 7 after 2% DSS administration. (**N**) Representative hematoxylin and eosin–stained sections of distal colon tissue from control mice not subjected to DSS (non-DSS) or control or *Sp140* knockdown mice subjected to 3.5% DSS for 7 days. Scale bar, 50 μm. (**O**) Histologic scores (0 to 6) for inflammation in colon tissue. Box-and-whisker plots show the mean and interquartile range for each condition. $*P < 0.05$, $**P < 0.01$, $***P < 0.001$, and $****P < 0.0001$, two-tailed unpaired t test [for (C) and (G) and (I) to (M)], two-way ANOVA [for (B), (E), and (F)], or one-way ANOVA [for (O)].

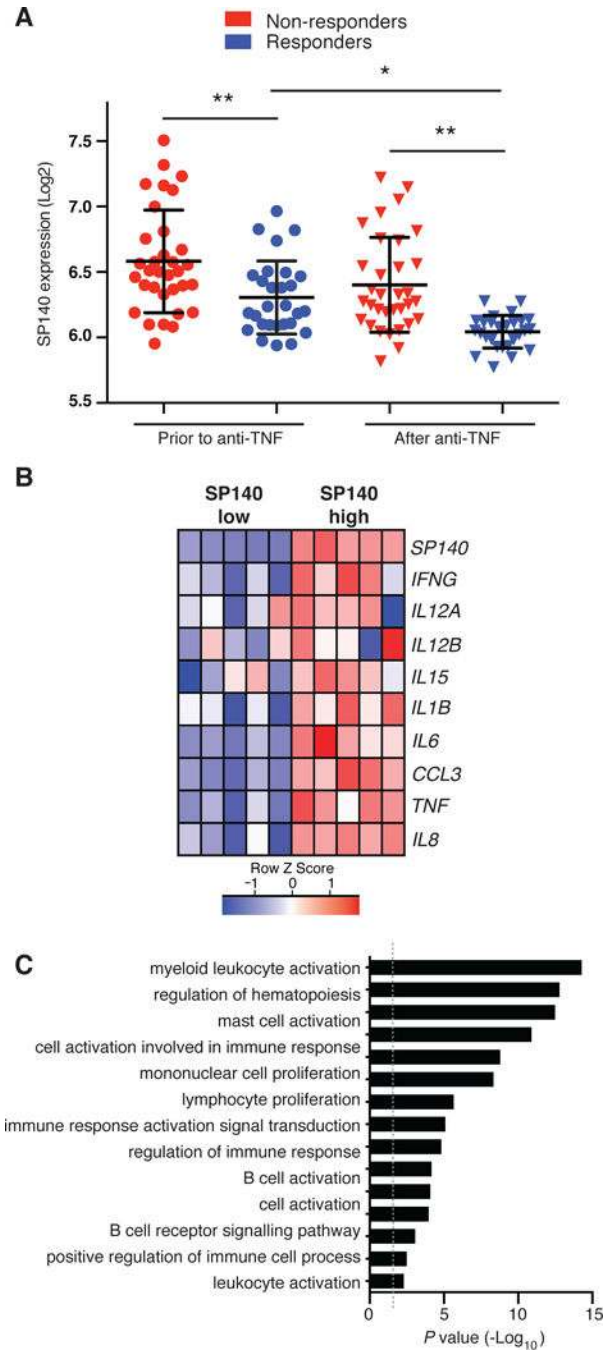

Fig. 8. Lower expression of *SP140* in intestinal biopsies significantly correlates with improved response to anti-TNF therapy

(**A**) Microarray expression of *SP140* in colonic biopsies from 19 CD and 24 ulcerative colitis patients before or 4 to 6 weeks after intravenous infusion of anti-TNF (infliximab). Patients were categorized as responders (blue) or nonresponders (red) to anti-TNF, as per criteria described (50). $*P < 0.05$ and $**P < 0.01$, one-way ANOVA, Tukey's multiple comparisons test. Error bars are SEM. (**B**) Microarray expression of indicated cytokines and chemokines in intestinal biopsies with high or low expression of *SP140*. (**C**) PANTHER

biological processes statistically overrepresented ($P < 0.01$) in genes whose expression positively correlates with *SP140* expression ($r^2 > 0.75$) in colonic biopsies of 19 CD and 24 ulcerative colitis patients.